# Proteomic Analysis of Potential Keratan Sulfate, Chondroitin Sulfate A, and Hyaluronic Acid Molecular Interactions

*Abigail H. Conrad,*[1,2] *Yuntao Zhang,*[1,2] *Elena S. Tasheva,*[1] *and Gary W. Conrad*[1]

**Purpose.** Corneal stroma extracellular matrix (ECM) glycosaminoglycans (GAGs) include keratan sulfate (KS), chondroitin sulfate A (CSA), and hyaluronic acid (HA). Embryonic corneal keratocytes and sensory nerve fibers grow and differentiate according to chemical cues they receive from the ECM. This study asked which of the proteins that may regulate keratocytes or corneal nerve growth cone immigration interact with corneal GAGs.

**Methods.** Biotinylated KS (bKS), CSA (bCSA), and HA (bHA) were prepared and used in microarray protocols to assess their interactions with 8268 proteins and a custom microarray of 85 extracellular epitopes of nerve growth-related proteins. Surface plasmon resonance (SPR) was performed with bKS and SLIT2, and their $k_a$, $k_d$, and $K_D$ were determined.

**Results.** Highly sulfated KS interacted with 217 microarray proteins, including 75 kinases, several membrane or secreted proteins, many cytoskeletal proteins, and many nerve function proteins. CSA interacted with 24 proteins, including 10 kinases and 2 cell surface proteins. HA interacted with 6 proteins, including several ECM-related structural proteins. Of 85 ECM nerve-related epitopes, KS bound 40 proteins, including SLIT, 2 ROBOs, 9 EPHs, 8 Ephrins (EFNs), 8 semaphorins (SEMAs), and 2 nerve growth factor receptors. CSA bound nine proteins, including ROBO2, 2 EPHs, 1 EFN, two SEMAs, and netrin 4. HA bound no ECM nerve-related epitopes. SPR confirmed that KS binds SLIT2 strongly. The KS core protein mimecan/osteoglycin bound 15 proteins.

**Conclusions.** Corneal stromal GAGs bind, and thus could alter the availability or conformation of, many proteins that may influence keratocyte and nerve growth cone behavior in the cornea. (*Invest Ophthalmol Vis Sci.* 2010;51:4500–4515) DOI: 10.1167/iovs.09-4914

Glycosaminoglycans (GAGs) are long, unbranched polysaccharide chains composed of repeating disaccharide units, often either D-glucuronic acid (GlcA), L-iduronic acid (IdoA), or D-galactose (Gal) linked to either D-*N*-acetylglucosamine (GlcNAc) or D-*N*-acetylgalactosamine (GalNAc). One or both sugars can be sulfated. The carboxylate ($-COO^-$) and sulfate ($-SO_4^{=}$) groups make GAGs highly negatively charged polymers. When most GAG chains are synthesized, they are covalently linked at their reducing end to core proteins, thus forming proteoglycans (PGs). The adult human corneal stroma contains (by weight) 65% keratan sulfate (KS) and 30% chondroitin/dermatan sulfate (CS/DS),[1] first identified as major GAGs of the cornea by Meyer et al.[2,3] Corneal KS chains are attached to the core proteins lumican, keratocan, and mimecan/osteoglycin,[4–6] and corneal CS/DS chains are attached to decorin and biglycan.[7,8] In addition, corneal stromal cells in culture,[9] early embryonic corneal endothelial cells,[10] and anterior stromal cells in injured adult corneas[11] also make hyaluronic acid (HA), unique among GAGs because it is neither covalently attached to a core protein nor sulfated.

GAGs influence many biological functions, including cell division, differentiation, signal transduction, adhesion, migration, peripheral nerve extension or regeneration, and responses to growth factors,[12–16] sometimes affecting cell adhesion and/or proliferation differently in different ECM compositions.[17] In exerting these influences, GAGs interact with proteins in many different ways. Clusters of basic amino acids in BBXB and BBBXXB sequences (where B is a basic amino acid and X is a hydrophilic amino acid) have been proposed as consensus GAG binding sites in some proteins.[18] In other cases, interactions between GAGs and proteins appear to be more directly charge-dependent, either because the degree of sulfation of the GAG determines the strength of the interaction,[19] or because an increase in the number of GAG chains on a core protein increases the interactions of that PG with other proteins.[20]

Little is known about the protein interactions of the corneal GAGs KS, CSA, and HA. KS, composed of repeating -[3Gal$\beta$1–4GlcNAc$\beta$1]- disaccharide units, has an average molecular mass of approximately 15 kDa. In addition to corneal core KS proteins, KS can be attached to fibromodulin, aggrecan, and PRELP in cartilage and to osteoadherin in bone.[21] Although often an ECM component, KS can also be on cell surfaces[22,23] or in the cytosol.[24] KS chains are sulfated to different degrees in different tissues,[25] at different stages of development within a given tissue,[26] and in different disease states.[27] KS chains bind the cardiotoxins CTX A3 and T$\gamma$[28] and insulin-like growth factor binding protein-2 (IGFBP2).[29] KS core proteins keratocan and lumican bind CXC chemokine KC during corneal inflammatory response.[30] No binding partners for mimecan/osteoglycin have been reported.

CS is composed of repeating -[4GlcA$\beta$1–3GalNAc$\beta$1]- disaccharide units, with sulfate groups covalently attached to C-4 of GalNAc (CSA), C-6 of GalNAc (CSC), C-2 of GlcA and C-6 of GalNAc (CSD), or C-4 and C-6 of GalNAc (CSE).[3] CS GAGs average approximately 21.5 kDa in molecular mass, can be

From the [1]Division of Biology, Kansas State University, Manhattan, Kansas.

[2]These authors contributed equally to the work presented here and should be regarded as equivalent authors.

Supported by a National Institutes of Health (NIH) Microarray Supplement Grant 3R01EY000952–35S1 to NIH 5R01EY000952, and NIH 2 R01EY000952 (GWC). The content of this paper is solely the responsibility of the authors and does not necessarily represent the official views of the National Eye Institute or the National Institutes of Health.

Submitted for publication November 12, 2009; revised January 19 and March 12, 2010; accepted March 19, 2009.

Disclosure: **A.H. Conrad**, None; **Y. Zhang**, None; **E.S. Tasheva**, None; **G.W. Conrad**, None

Corresponding author: Abigail H. Conrad, Division of Biology, Ackert Hall, Kansas State University, Manhattan, KS 66506-4901; aconrad@ksu.edu.



Investigative Ophthalmology & Visual Science, September 2010, Vol. 51, No. 9

sulfated to different degrees in different tissues, and are linked to core proteins. Sulfated CS binds the secreted growth factor Nodal.[31] CSA binds opticin (OPT)[32] and Indian hedgehog,[33] but not pleiotrophin,[34] FGF-3, -5, -6, -8, -22,[35] or BMP4.[36]

Nonsulfated anionic HA, first discovered in ocular vitreous humor,[37] is composed of repeating -[4GlcA$\beta$1–3GlcNAc$\beta$1]- disaccharide units, is synthesized on the plasma membrane with no attachment to any core protein, and is very large, with molecular masses from 100 to 10,000 kDa. Nonsulfated HA has the same chemical composition in any tissue in which it occurs. HA noncovalently binds several PGs (aggrecan,[38] versican,[39] neurocan,[40] and brevican[41]), link proteins,[42] TNF-stimulated gene 6 (TSG-6),[43] and the receptor CD44[44] through a linking region known as the PG tandem repeat (PTR) module.[45] Other HA-binding proteins include fibronectin,[46] receptor for HA-mediated mobility (RHAMM),[47,48] and intracellular adhesion molecule-1 (ICAM-1).[49] There is increasing evidence that HA occurs intracellularly,[50,51] as well as extracellularly.

In developing chick embryos, the neurorepellant ECM component semaphorin 3A (SEMA3A), secreted by the lens, strongly influences when neural crest–derived corneal peripheral nerve axons invade the corneal anterior stroma and extend and branch through the anterior stroma and corneal epithelium.[52] Corneal nerve growth cone penetration occurs, even though anterior stromal cells and corneal epithelial cells express SLIT2, a strong negative regulator of nerve growth, throughout chick embryonic development.[53,54] It has been suggested that, in the posterior E9 cornea, ECM-accumulated, highly sulfated KS binds and thereby blocks the diffusion of lens SEMA3A, thus allowing anterior stromal penetration of corneal nerve growth cones to begin on E9, and that corneal nerves extend into the anterior stroma and eventually into the corneal epithelium, to avoid increasing ECM accumulation of highly sulfated KS from posterior to anterior in the developing corneal stroma.[53]

To test this hypothesis and identify other proteins that may interact with corneal GAGs, bovine corneal KS, sturgeon notochord CSA, and chicken cockscomb HA were biotinylated and used to screen an Invitrogen Proteomics Array of more than 8000 intracellular and extracellular (Version 4 [v4]; Invitrogen, Carlsbad, CA) proteins and a separate custom array of 85 extracellular epitopes of neuroregulator receptors, ligands, and growth factors. The biotinylated corneal KS core protein mimecan (OGN) was also used to screen the v4 array. The least prevalent corneal KS core protein by % weight, it may play a major role in some functions, depending on its localization, and nothing is currently known about the proteins that it may bind. Corneal KS, sturgeon notochord CSA, and HA bound many of these proteins selectively, suggesting that KS, CSA, and HA could alter the availability or conformation of many proteins that may influence corneal keratocyte and nerve growth cone behavior.

## METHODS

### Materials

Bovine corneal KS and sturgeon notochord CSA were purchased from Northstar BioProducts of Associates of Cape Cod, Inc. (ACC; formerly Seikagaku America; East Falmouth, MA). Biotinylated chicken cockscomb HA (bHA), *N*-ethyl-*N*′-(3-dimethylaminopropyl)-carbodiimide (EDC), and biotin-X-hydrazide were purchased from Sigma-Aldrich (St. Louis, MO). MES-buffered saline packs (BupH) and the biotin quantitation assay contained in a biotinylation kit (EZ-Link Sulfo-NHS-LC-Biotinylation Kit; product no. 21435) were purchased from Thermo Scientific Pierce Protein Research Products (Rockford, IL). A centrifugal filter (regenerated cellulose 3000 MWCO; Ambion Ultra) was purchased from Millipore Biomanufacturing and Life Research Products (Billerica, MA). Protoarray v4 proteins, Alexa-Fluor 647-labeled goat anti-rat IgG, V5-his-tagged calmodulin kinase 1, and Alexa-Fluor 647-labeled anti-V5 antibody were supplied by Invitrogen as part of their protoarray service. All extracellular epitopes of nerve-related proteins listed in Table 1, mimecan protein, and rat anti-mouse mimecan antibody were pur-

**TABLE 1.** Protein Epitopes Used in Nerve-Related Protoarray

| Protein | Symbol | With $IgG_1$ | Without $IgG_1$ |
|---|---|---|---|
| Human $IgG_1$ Pro100-Lys330 | | X | |
| Human Integrin alpha V beta 3 | $\alpha V\beta 3$ | | # |
| Human Integrin alpha 3 beta 1 | $\alpha 3\beta 1$ | | # |
| Human FGF acidic | FGFa | | # |
| Human FGF basic (157 aa), | FGFb | | # |
| Human EGF | EGF | | # |
| Human PDGF | PDGF | | # |
| Human TGF-beta 1 | TGF$\beta$1 | | # |
| Human NT-3 | NT3 | | # |
| Human TrkA | Ntrk1 | X | X |
| Human TrkB | Ntrk2 | | # |
| Human TrkC | Ntrk3 | X | X |
| Human NGFR/TNFRSF16 | NGFR | | X |
| Human Neuregulin-1, SMDF isoform | NRG1 | | # |
| Human ErbB2 | ERBB2 | X | X |
| Human ErbB4 | ERBB4 | X | X |
| Mouse SLIT3 | SLIT3 | | # |
| Rat ROBO1 | ROBO1 | X | X |
| Human ROBO2 | ROBO2 | X | X |
| Mouse Ephrin-A1 | EFNA1 | X | X |
| Mouse Ephrin-A2 | EFNA2 | X | X |
| Human Ephrin-A3 | EFNA3 | X | X |
| Human Ephrin-A4 | EFNA4 | X | X |
| Human Ephrin-A5 | EFNA5 | X | X |
| Mouse Ephrin-B1 | EFNB1 | X | X |
| Mouse Ephrin-B2 | EFNB2 | X | X |
| Human Ephrin-B3 | EFNB3 | X | X |
| Human EphA1 | EPHA1 | X | X |
| Mouse EphA2 | EPHA2 | X | X |
| Mouse EphA3 | EPHA3 | X | X |
| Mouse EphA4 | EPHA4 | X | X |
| Rat EphA5 | EPHA5 | X | X |
| Mouse EphA6 | EPHA6 | X | X |
| Mouse EphA7 | EPHA7 | X | X |
| Mouse EphA8 | EPHA8 | X | X |
| Rat EphB1 | EPHB1 | X | 0 |
| Mouse EphB2 | EPHB2 | X | X |
| Mouse EphB3 | EPHB3 | X | 0 |
| Mouse EphB4 | EPHB4 | X | X |
| Mouse EphB6 | EPHB6 | X | X |
| Human Semaphorin 3A | SEMA3A | X | 0 |
| Human Semaphorin 3E | SEMA3E | | # |
| Mouse Semaphorin 3F (Trunc) | SEMA3F | X | X |
| Human Semaphorin 4A | SEMA4A | X | 0 |
| Human Semaphorin 6A | SEMA6A | X | X |
| Human Semaphorin 6B | SEMA6B | X | X |
| Human Neuropilin-1 | NPN1 | | # |
| Human Neuropilin-2 | NPN2 | X | X |
| Chicken Netrin-1 | NTN1 | | # |
| Chicken Netrin-2 | NTN2 | | # |
| Human Netrin-4 | NTN4 | | # |
| Mouse DCC | DCC | X | |
| Rat UNC5H1 | NC5H1 | X | |
| Rat UNC5H2 | NC5H2 | X | |
| Human UNC5H3 | UNC5H3 | X | |
| Human UNC5H4 | NC5H4 | X | |

Total number of proteins = 85. X, incorporated in protoarray; #, incorporated in protoarray, but only available without $IgG_1$ fusion; 0, no $IgG_1$ cleaved form available.

**Table 2.** Proteins that Interact with Highly Sulfated Keratan Sulfate GAG Chains

| Protein | Signal | Database ID | Invitrogen ID | Protein Description |
|---|---|---|---|---|
| ABL1 | 43,459 | NP_005148.2 | P3049 | v-abl Abelson murine leukemia viral oncogene homologue 1 |
| DNAJC8 | 41,722 | NP_055095.2 | NM_014280.1 | DnaJ (Hsp40) homologue, subfamily C, member 8 |
| PQBP1 | 39,994 | NP_005701.1 | NM_005710.1 | Polyglutamine binding protein 1 |
| ABL1 | 38,005 | NP_005148.2 | PV3864 | v-abl Abelson murine leukemia viral oncogene homologue 1, E255K |
| RPS6KB2 | 37,356 | NP_003943 | PV3831 | Ribosomal protein S6 kinase, 70kDa, polypeptide 2 |
| TBK1 | 37,330 | NP_037386.1 | PV3504 | TANK-binding kinase 1 |
| PLK1 | 36,949 | NP_005021.2 | PV3501 | Polo-like kinase 1 (Drosophila) |
| ABL1 | 36,821 | NP_005148.2 | PV3866 | v-abl Abelson murine leukemia viral oncogene homologue 1, T351I |
| CAPRIN1 | 35,834 | NP_005889.3 | NM_005898.4 | Cell cycle associated protein 1 |
| COL23A1 | 35,723 | NP_775736.2 | BC042428.1 | Collagen, type XXIII, alpha 1 |
| ABL1 | 35,400 | NP_005148.2 | PV3865 | v-abl Abelson murine leukemia viral oncogene homologue 1, G250E |
| AXL | 35,361 | NP_068713 | PV3971 | AXL receptor tyrosine kinase |
| NUAK1 | 35,266 | NP_055655.1 | PV4127 | NUAK family, SNF1-like kinase 1 |
| ABL1 | 38,005 | NP_005148.2 | PV3863 | v-abl Abelson murine leukemia viral oncogene homologue 1, Y253F |
| PDAP1 | 34,768 | NP_055706 | NM_014891.1 | PDGFA associated protein 1 |
| AFF4 | 34,570 | NP_055238.1 | BC025700.1 | AF4/FMR2 family, member 4 |
| CCDC43 | 34,393 | NP_653210 | BC047776.2 | Coiled-coil domain containing 43 |
| EPB49 | 34,349 | NP_001107608 | BC052805.1 | Dematin: erythrocyte membrane protein band 4.9 |
| CHUK | 34,299 | NP_001269 | PV4310 | Conserved helix-loop-helix ubiquitous kinase |
| F11R | 34,234 | NP_058642.1 | NM_016946.3 | F11 receptor |
| CDC2 | 34,115 | NP_001777.1 | PV3292 | Cell division cycle 2, G1 to S and G2 to M |
| MYLK2 | 32,835 | NP_149109.1 | PV3757 | Myosin light chain kinase 2, skeletal muscle |
| RAD51AP1 | 32,494 | NP_006470.1 | NM_006479.2 | RAD51 associated protein 1 |
| CCNT1 | 32,383 | NP_001231 | PV4131 | Cyclin T1 |
| KCNAB2 | 32,108 | NP_003627.1 | NM_003636.1 | Potassium voltage-gated channel, shaker-related subfamily, beta 2 |
| KIT V654A | 31,817 | NP_000213 | PV4132 | v-kit Hardy-Zuckerman 4 feline sarcoma viral oncogene homologue |
| DIDO1 | 31,785 | NP_149072.1 | BC000770.1 | Death inducer-obliterator 1 |
| RPS6KA1 | 31,745 | NP_002944.2 | PV3680 | Ribosomal protein S6 kinase, 90kDa, polypeptide 1 |
| CCDC55 | 31,679 | NP_115517.1 | NM_032141.1 | Coiled-coil domain containing 55 |
| ADD2 | 31,550 | NP_059522.1 | BC065525.1 | Adducin 2 (beta) |
| PRR15 | 31,499 | NP_787083 | NM_175887.2 | Proline rich 15 |
| BTK | 31,423 | NP_000052 | PV3363 | Bruton agammaglobulinemia tyrosine kinase |
| ITGA6 | 31,406 | NP_000201.2 | NM_000210.1 | Integrin alpha 6 |
| PHF15 | 31,163 | NP_056103 | BC00492.1 | PHD finger protein 15 |
| UBE2S | 31,160 | NP_055316 | BC004236.2 | Ubiquitin-conjugating enzyme E2S |
| RPS6KA2 | 30,817 | NP_066958.2 | PV3846 | Ribosomal protein S6 kinase, 90kDa, polypeptide 2 |
| STK25 | 30,743 | NP_006365.2 | PV3657 | Serine/threonine kinase 25 (STE20 homologue, yeast) |
| HSPC148 | 30,545 | NP_057487.2 | BC040946.1 | CWC 15 homologue (S. cerevisiae) |
| MAP2 | 30,395 | NP_002365.3 | NM_031845.1 | Microtubule-associated protein 2 |
| NTRK3 | 30,375 | NP_002521 | PV3617 | Neurotrophic tyrosine kinase, type 3 |
| BMX | 30,146 | NP_001712 | PV3371 | BMX non-receptor tyrosine kinase |
| NEK2 | 29,418 | NP_002488 | PV3360 | NIMA (never in mitosis gene a)-related kinase 2 |
| NEK3 | 29,363 | NP_689933 | PV3821 | NIMA (never in mitosis gene a)-related kinase 3 |
| ARHGAP17 | 29,340 | NP_001006635.1 | NM_001006634.1 | Rho GTPase activating protein 17 |
| DAPK2 | 29,080 | NP_055141.2 | PV3614 | Death-associated protein kinase 2 |
| MAP2K2 | 29,037 | NP_109587.1 | PV3615 | Mitogen-associated protein kinase kinase 2 |
| UBXD3 | 28,418 | NP_689589 | NM_152376.2 | UBX domain containing 3 |
| PAK4 | 28,292 | NP_005875.1 | NM_005884.2 | p21(CDKN1A)-activated kinase 4 |
| ANKRD50 | 27,779 | NP_065070 | BC024725.1 | Ankyrin repeat domain 50 |
| ABL2 | 27,620 | NP_009298.1 | PV3266 | v-abl Abelson murine leukemia viral oncogene homologue 2 |
| CACNB1 | 27,417 | NP_000714.3 | NM_000723.3 | Calcium channel, voltage-dependent, beta 1 subunit |
| TSSK2 | 27,281 | NP_443732.3 | PV3622 | Testis-specific serine kinase 2 |
| SCEL | 27,277 | NP_659001.1 | BC020726.1 | Sciellin |
| SERBP1 | 27,009 | NP_001018077.1 | BC003049.1 | SERPINE1 mRNA binding protein |
| RPS6KA4 | 26,944 | NP_003933 | PV3782 | Ribosomal protein S6 kinase, 90kDa, polypeptide 4 |
| TBC1D10C | 26,829 | NP_940919.1 | NM_198517.2 | TBC1 domain family, member 10C |
| KIAA1706 | 26,773 | NP_085139.2 | NM_030636.1 | KIAA1706 protein |
| WIBG | 26,756 | NP_115721.1 | NM_032345.1 | Within bgcn homologue (Drosophila) |
| E2F8 | 26,667 | NP_078956.2 | BC028244.1 | E2F transcription factor 8 |
| FKBP3 | 26,667 | NP_002004 | NM_002013.2 | FK506 binding protein 3 |
| TCEAL2 | 26,595 | NP_525129 | NM_080390.3 | Transcription elongation factor A (SII)-like 2 |
| VRK3 | 26,225 | NP_057524.3 | NM_016440.1 | Vaccinia related kinase 3 |
| AURKB | 25,925 | NP_004208.2 | PV3970 | Aurora kinase B |
| STK24 | 25,564 | NP_003567.2 | PV3560 | Serine/threonine kinase 24 (STE20 homologue, yeast) |
| CSNK1G2 | 25,425 | NP_001310.3 | PV3499 | Casein kinase 1, gamma 2 |
| DAPK3 | 25,279 | NP_001339 | PV3686 | Death-associated protein kinase 3 |
| DCX | 25,123 | NP_835365.1 | NM_178152.1 | Doublecortin: Doublecortex; lissencephaly, X-linked |
| SMITH | 25,068 | NP_066972.1 | Smith | SMITH antigen (Sm) |

(*continues*)

**TABLE 2** (*continued*). Proteins that Interact with Highly Sulfated Keratan Sulfate GAG Chains

| Protein | Signal | Database ID | Invitrogen ID | Protein Description |
|---|---|---|---|---|
| SCYE1 | 24,980 | NP_001135887.1 | BC01451.1 | Small inducible cytokine subfamily E, member 1, endothelial monocyte activating |
| PRKG2 | 24,956 | NP_006250.1 | PV3973 | Protein kinase, cGMP-dependent, type II |
| PRR16 | 24,762 | NP_057728.1 | BC038838.1 | Proline rich 16 |
| DDX42 | 24,754 | NP_031398.2 | BC015505.1 | DEAD (Asp-Glu-Ala-Asp) box polypeptide 2 |
| NEK4 | 24,659 | NP_003148.2 | PV4315 | NIMA (never in mitosis gene a)-related kinase 4 |
| TTK | 24,534 | NP_003309.2 | PV3792 | TTK protein kinase |
| WWP2 | 24,484 | NP_008945.2 | BC000108.1 | WW domain containing E3 ubiquitin protein ligase 2 |
| ARPP-19 | 24,474 | NP_006619.1 | NM_006628.4 | Cyclic AMP phosphoprotein, 19kD |
| CSNK1E | 24,328 | NP_001885.1 | PV3500 | Casein kinase 1, epsilon |
| ABLIM1 | 24,223 | NP_002304.3 | BC002448.2 | Actin binding LIM protein 1 |
| MAP2K6 | 24,152 | NP_002749.2 | PV3318 | Mitogen-associated protein kinase kinase 6 |
| PAK1 | 23,993 | NP_002567 | PV3820 | p21/Cdc42/Rac1-activated kinase 1 (STE20 homologue, yeast) |
| ANKS4B | 23,921 | NP_665872.2 | NM_145865.1 | Ankyrin repeat and sterile alpha motif domain containing 4B |
| DCAMKL2 | 23,892 | NP_689832 | PV4297 | Doublecortin and CaM kinase-like 2 |
| ZNF706 | 23,792 | NP_057180.1 | NM_016096.1 | Zinc finger protein 706 |
| IRS1 | 23,732 | NP_005535.1 | BC053895.1 | Insulin receptor substrate 1 |
| FAM128A | 23,684 | NP_001078834.1 | BC018206.1 | Family with sequence similarity 128, member A |
| ACTR1B | 23,582 | NP_005726.1 | NM_005735.2 | Centractin beta (yeast): actin-related protein homologue B |
| KIAA1143 | 23,465 | NP_065747.1 | BC016790.1 | KIAA1143 |
| CTNNA1 | 23,428 | NP_001894.2 | BC031262.1 | Catenin (cadherin-associated protein), alpha 1, 102kDa |
| EPHA2 | 23,315 | NP_004422.2 | PV3688 | Ephrin receptor A2 |
| HOMER2 | 23,290 | NP_004830.2 | BC012109.1 | Homer homologue 2 (Drosophila) |
| NTRK2 | 23,143 | NP_006171 | PV3616 | Neurotrophic tyrosine kinase, receptor, type 2 |
| TCP10L | 23,126 | NP_653260.1 | NM_144659.1 | t-complex 10 (mouse)-like |
| LIMCH1 | 22,817 | NP_055803.2 | BC023546.2 | LIM and calponin homology domains 1 |
| YES1 | 22,580 | NP_005424.1 | P3078 | v-yes-1 Yamaguchi sarcoma viral oncogene homologue 1 |
| EIF5 | 22,457 | NP_001960.2 | BC032866.2 | Eukaryotic translation initiation factor 5 |
| KIF2C | 22,401 | NP_006836.2 | BC014924.1 | Kinesin family member 2C |
| EIF3S4 | 22,358 | NP_003746.2 | BC014924.1 | Eukaryotic translation initiation factor 3, subunit G |
| SRPK1 | 22,335 | NP_003128.3 | PV4215 | SFRS protein kinase 1 |
| TRPT1 | 22,333 | NP_113660.1 | NM_031472.1 | tRNA phosphotransferase 1 |
| SMTNL2 | 22,279 | NP_940903.2 | NM_198501.1 | Smoothelin-like 2 |
| LARP4 | 22,254 | NP_954658.1 | NM_199188.1 | La ribonucleoprotein domain family, member 4 |
| NMT1 | 22,231 | NP_066565.1 | NM_021079.2 | N-myristoyltransferase 1 |
| DAP | 22,223 | NP_004385.1 | NM_004394.1 | Death-associated protein |
| MAPRE1 | 22,209 | NP_036457.1 | NM_012325.1 | Microtubule-associated protein, RP/EB family, member 1 |
| CSNK1G3 | 22,208 | NP_004375.2 | PV3838 | Casein kinase 1, gamma 3 |
| NTRK1 | 22,192 | NP_002520.2 | PV3134 | Neurotrophic tyrosine kinase, receptor, type 1 |
| KIF3B | 22,121 | NP_004789.1 | NM_004798.2 | Kinesin family member 3B |
| EBAG9 | 21,974 | NP_004206.1 | NM_004215.2 | Estrogen receptor binding associated, antigen 9 |
| FGFR1OP | 21,817 | NP_008976.1 | NM_007045.2 | FGFR1 oncogene partner |
| NPM1 | 21,797 | NP_002511.1 | BC021983.1 | Numatrin: nucleophosmin (nucleolar phoshoprotein B23) |
| LARP6 | 21,777 | NP_060827.2 | NM_018357.2 | La ribonucleoprotein domain family, member 6 |
| LYN | 21,548 | NP_002341.1 | P2907 | v-yes-1 Yamaguchi sarcoma viral oncogene homologue |
| RTF1 | 21,542 | NP_055953.3 | NM_105138.2 | Rtfl, Paf1/RNA polymerase II complex component, homolog |
| FES | 21,524 | NP_001996.1 | PV3354 | Feline sarcoma oncogene |
| HMGB1 | 21,497 | NP_002119.1 | NM_002128.2 | High-mobility group box 1 |
| SLC4A1AP | 21,473 | NP_060628.2 | NM_018158.1 | Solute carrier family 4 (anion exchanger) member 1, adaptor protein |
| NMT2 | 21,461 | NP_004799.1 | BC006376.1 | N-myristoyltransferase 2 |
| G3BP1 | 21,423 | NP_938405.1 | NM_198395.1 | GTPase activating protein (SH3 domain) binding protein 1 |
| IRAK4 | 21,417 | NP_057207 | PV3362 | Interleukin-1 receptor-associated kinase 4 |
| PSRC1 | 21,391 | NP_116025.1 | NM_032636.2 | Proline/serine-rich coiled-coil 1 |
| RBM8A | 21,196 | NP_005096.1 | NM_005105.2 | RNA binding motif protein 8A |
| EPHA8 | 21,107 | NP_065387 | PV3844 | Ephrin receptor A8 |
| LMNA | 21,093 | NP_733821.1 | BC033088.1 | Lamin A/C |
| SYTL2 | 20,914 | NP_116561.1 | NM_032943.2 | Synaptotagmin-like 2 |
| TSSK1B | 20,661 | NP_114417 | PV3505 | Testis-specific serine kinase 1B |
| RGS14 | 20,566 | NP_006471.2 | NM_006480.4 | Regulator of G-protein signaling 14 |
| AURKA | 20,210 | NP_940839 | PV3612 | Aurora kinase A |
| NKIRAS1 | 19,916 | NP_065078.1 | NM_020345.3 | NFKB inhibitor interacting RAS-like 1 |
| PPID | 19,915 | NP_005029.1 | NM_005038.1 | Cyclophilin D: peptidylprolyl isomerase D |
| MARK4 | 19,852 | NP_113605 | PV3851 | MAP/microtubule affinity-regulating kinase 4 |
| NEK1 | 19,713 | NP_006613 | PV4202 | NIMA (never in mitosis gene a)-related kinase 1 |
| LENG1 | 19,379 | NP_077292.1 | NM_024316.1 | Leukocyte receptor cluster member 1 |
| SETBP1 | 19,196 | NP_056374.2 | BC062338.1 | SET binding protein 1 |
| PPP1R8 | 19,041 | NP_054829.2 | NM_014110.3 | Protein phosphatase 1, regulatory (inhibitor) subunit 8 |
| CFDP1 | 18,952 | NP_006315.1 | NM_006324.1 | Craniofacial development protein 1 |

(*continues*)

**TABLE 2** (*continued*). Proteins that Interact with Highly Sulfated Keratan Sulfate GAG Chains

| Protein | Signal | Database ID | Invitrogen ID | Protein Description |
|---|---|---|---|---|
| DDX19B | 18,769 | NP_009173.1 | NM_007242.3 | DEAD (Asp-Glu-Ala-Asp) box polypeptide 19B |
| ZAK | 18,704 | NP_598407 | PV3882 | Sterile alpha motif and leucine zipper containing kinase AZK |
| ASXL1 | 18,629 | NP_056153.2 | BC064984.1 | Additional sex-combs like 1 (Drosophila) |
| FGFR1 | 18,588 | NP_000595 | PV3146 | Fibroblast growth factor receptor 1 (fms-related tyrosine kinase 2) |
| ERBB2 | 18,556 | NP_004439 | PV3366 | v-erb-b2; neuro/glioblastoma derived oncogene homologue (avian) |
| PTK2B | 18,455 | NP_775266.1 | BC036651.2 | Protein tyrosine kinase 2 beta |
| DDX54 | 18,433 | NP_001104792.1 | BC001131.1 | DEAD (Asp-Glu-Ala-Asp) box polypeptide 54 |
| MEOX1 | 18,335 | NP_004518.1 | NM_004527.2 | Mesenchyme homeobox 1 |
| OCEL1 | 18,291 | NP_078854.1 | NM_024578.1 | Occludin/ELL domain containing 1 |
| ING5 | 18,217 | NP_115705.2 | NM_032329.4 | Inhibitor of growth family, member 5 |
| ASXL2 | 18,195 | NP_060733.4 | BC042999.2 | Additional sex-combs like 2 (Drosophila) |
| TFPT | 18,176 | NP_037474.1 | BC001728.1 | TCF3 (E2A) fusion partner (in childhood leukemia) |
| IFRD2 | 18,021 | NP_006755.4 | BC001327.1 | Interferon-related developmental regulator 2 |
| MARK2 | 17,836 | NP_059672.2 | PV3878 | MAP/microtubule affinity-regulating kinase 2 |
| SIRPG | 17,784 | NP_061026.2 | BC064532.1 | Signal-regulatory protein gamma |
| KDR | 17,770 | NP_002244 | PV3660 | Kinase insert domain receptor (a type III receptor tyrosine kinase) |
| MRPL1 | 17,755 | NP_064621.3 | BC015109.1 | Mitochondrial ribosomal protein L1 |
| RPAP3 | 17,682 | NP_078880.1 | BC056415.1 | RNA polymerase II associated protein 3 |
| FAM50A | 17,629 | NP_004690.1 | NM_004699.1 | Family with sequence similarity 50, member A |
| UBE2E2 | 17,443 | NP_689866.1 | NM_152653.1 | Ubiquitin-conjugating enzyme E2E 2 |
| CDKN1B | 17,376 | NP_004055.1 | NM_004064.2 | Cyclin-dependent kinase inhibitor 1B (p27, Kip1) |
| PKN2 | 17,294 | NP_006247 | PV3879 | Protein kinase N2 |
| LIG3 | 17,224 | NP_039269.2 | NM_013975.1 | Ligase III, DNA, ATP-dependent |
| MESDC2 | 17,222 | NP_055969.1 | BC012746.1 | Mesoderm development candidate 2 |
| TRUB1 | 17,203 | NP_631908.1 | NM_139169.2 | TruB pseudouridine (psi) synthetase homologue 1 |
| MAPKAPK3 | 17,148 | NP_004626.1 | BC001662.1 | Mitogen-activated protein kinase-activated protein kinase 3 |
| SRC | 17,080 | NP_005408 | P3044 | v-src sarcoma (Schmidt-Ruppin A-2) viral oncogene homologue |
| BAIAP2 | 16,925 | NP_059344.1 | BC014020.1 | BAI1-associated protein 2 |
| STAC | 16,897 | NP_003140.1 | BC020221.1 | SH3 and cystein rich domain |
| TPPP | 16,891 | NP_008961.1 | NBM_007030.1 | Tubulin polymerization promoting protein |
| FMNL1 | 16,811 | NP_005883.2 | BC021906.1 | Formin-like 1 |
| HMGN1 | 16,811 | NP_004956.5 | NM_004965.3 | High-mobility group nucleosome binding domain 1 |
| GLB1L | 16,727 | NP_078782.3 | NM_024506.3 | Galactosidase, beta 1-like |
| FLT3 | 16,478 | NP_004110 | PV3967 | Fms-related tyrosine kinase 3 |
| PIP4K2C | 16,448 | NP_079055.3 | NM_024779.2 | Phosphotidylinositol-5-phosphaste 4-kinase, type II, gamma |
| GSK3B | 16,258 | NP_002084 | PV3365 | Glycogen synthetase kinase 3 beta |
| ODF2 | 16,221 | NP_002531.3 | BC010629.1 | Outer dense fiber of sperm tails 2 |
| ZHX2 | 16,169 | NP_055758.1 | NM_014943.3 | Zinc fingers and homeoboxes 2 |
| DNM2 | 16,068 | NP_001005360.1 | BC054401.1 | Dynamin 2 |
| LAD1 | 16,058 | NP_005549.2 | NM_005558.2 | Ladinin 1 |
| COASY | 16,042 | NP_001035994.1 | BC020985.1 | Coenzyme A synthetase |
| BRD3 | 15,978 | NP_031397.1 | BC032124.1 | Bromodomain containing 3 |
| HCK | 15,939 | NP_002101 | P2908 | Hemopoietic cell kinase |
| EFCAB4A | 15,902 | NP_775855.3 | BC033196.1 | EF-hand calcium binding domain 4A |
| MAP3K10 | 15,869 | NP_002437 | PV3877 | Mitogen-activated protein kinase kinase kinase 10 |
| BCAR3 | 15,837 | NP_003558.1 | BC039895.1 | Breast cancer anti-estrogen resistance 3 |
| COIL | 15,815 | NP_004636.1 | NM_004645.1 | Coilin |
| PCDHGC3 | 15,791 | NP_115779.1 | NM_032403.1 | Protocadherin gamma subfamily C, 3 |
| EPHA3 | 15,698 | NP_005224 | PV3359 | Ephrin receptor A3 |
| AMMECR1L | 15,601 | NP_113633.2 | NM_031445.1 | AMME chromosomal region gene 1 -like |
| ZMYM3 | 15,595 | NP_005087.1 | BC013009.1 | Zinc finger, MYM-type 3 |
| SEMA3A-Fc | 5,913 | NP_006071.1 | | Semaphorin 3A, extracellular domain |

$n$ = 217 of 8,268 screened.

chased from R&D Systems (Minneapolis, MN). Surface plasmon resonance (SPR) analysis was conducted on a commercial system (model 3000; GE Health Care; Biacore Life Sciences Division [GE/Biacore], Piscataway, NJ), and the data were analyzed (BIAevaluation software 4.1; GE/Biacore). Streptavidin (SA)-coated chips, biotin capture kits, and HEPES buffer HBS-P (with 0.005% [vol/vol] surfactant P20, 10 mM HEPES ([pH 7.4], 150 mM NaCl) running buffer were also purchased from GE/Biacore.

## Preparation of Biotinylated KS

Seikagaku America purified KS by chromatography and chondroitinase ABC treatment, leaving a residual core peptide at the reducing terminus of KS chains. The average molecular mass of the purified KS was approximately 15 kDa. Attachment of biotin to free carboxy groups in the residual core peptide was performed by using the EDC protocol.[55,56] KS (1 mg) was dissolved in 0.5 mL 0.1 M MES ((2-*N*-morpholino)ethanesulfonic acid; pH 4.5), containing 2 mg/mL biotin-LC-hydrazide and 20 mg/mL EDC. The mixture was rotated end-over-end at room temperature for 24 hours. With a centrifugal filter (regenerated cellulose 3000 MWCO, Amicon Ultra; Millipore), biotinylated KS (bKS) molecules were extensively washed with deionized $H_2O$ to remove salt and free biotin and then were lyophilized. The yield of bKS was 0.8 mg. The 2-(4′-hydroxyazobenzene) benzoic acid (HABA) assay was used for measuring the level of biotin incorporation according to the manufacturer's protocol (EZ-Link Sulfo-NHS-LC-Biotinylation Kit; Thermo Scientific). Briefly, a calibration curve was obtained by adding biotin to

500 μL avidin-HABA reagent and measuring the decrease in absorbance at 500 nm. The biotin content of bKS was estimated by mixing 50 μL of the sample and 450 μL of the avidin-HABA reagent and comparing the absorbance at 500 nm with the standard. A biotinylation ratio of 1.43 moles biotin per mole KS was obtained, suggesting that one to two molecules of biotin were attached to each KS chain. Since there are no free carboxyl groups in the KS disaccharide, no biotin molecules were attached along the sides of the KS chain.

## Preparation of Biotinylated CSA

Sturgeon notochord CSA was highly purified by chromatography by Seikagaku America. The average molecular mass of CSA was ~16 kDa. Purified CSA was labeled (EZ-link Biotin-LC-Hydrazide; Thermo Scientific), and biotin was attached to the carboxyl groups of uronic acid residues along the CSA GAG chain, by using the EDC protocol,[55,56] beginning with 2 mg CSA dissolved in 1 mL 0.1 M MES (pH 4.5) containing 2 mg/mL biotin-LC-hydrazide and 20 mg/mL EDC. The yield of the biotinylated CSA (bCSA) was 1.7 mg. The HABA assay was used to determine a biotinylation ratio of 2.78 moles biotin per mole CSA, which is equivalent to 7.6 residues of biotin for every 100 disaccharide residues.

## Biotinylated HA

Biotinylated chicken cockscomb HA (bHA) was purchased directly from Sigma-Aldrich. According to the certificate of analysis, the molecular mass of the HA was 850 kDa. Biotin was attached by the manufacturer to carboxyl groups of glucuronic acid along the HA GAG chain, resulting in a degree of substitution of 6 mol%, which is equivalent to 6 residues of biotin for every 100 disaccharide residues.

## GAG Protoarrays

Protoarray Version 4 (Invitrogen) comprises 8268 human proteins, most of which are produced in baculovirus expression systems as N-terminal glutathione *S*-transferase fusion proteins and purified using glutathione *S*-Sepharose under nondenaturing conditions. These proteins, therefore, do not carry any of the posttranslational modifications, such as glycosylation side chains, that they may carry when synthesized in their normal human cell environment. All proteins were dissolved in printing buffer (PB) (50 mM HEPES, 200 mM NaCl, 0.08% Triton X-100, 25% glycerol, and 20 mM reduced glutathione, pH 7.5) at ~50 ng/μL and spotted on nitrocellulose-coated glass slides. Protein purification and array printing were done at ~6°C. A searchable list of these proteins may be viewed at: http://hdl.handle.net/2097/1716, including the amino acid sequence of the protein version spotted at each site, an estimate of the amount of protein in each spot for all GST-tagged proteins, based on an assay with an anti-GST antibody, and an Invitrogen account number or uIOH number for each protein that can be used at Invitrogen's website to find additional information about that protein. Reproducibility of protein binding for a test ligand within a single v4 assay run was assessed as follows: (1) All proteins were spotted in duplicate at each location; (2) some v4 proteins were spotted at several different locations, either as slight variants containing small amino acid variations of other v4 proteins or as larger variants containing only partial sequences of the full-length protein whose name they bear in the searchable list; (3) some kinases, recognized by a uIOH number starting with P or PV, have His tags rather than GST tags, and generally adhered to the nitrocellulose-coated glass slides at higher concentrations than GST-tagged proteins. In conjunction with the KS v4 studies, a custom plate containing SEMA3A-Fc, spotted in duplicate in a four-step concentration gradient (5, 10, 20, and 40 ng/μL), was also prepared.

Printed plates were washed with PB and then blocked with SMI buffer (50 mM Tris [pH 7.5], 5 mM $Mg_2SO_4$, 0.1% Tween-20, and 1% BSA, with the 1% BSA acting as the blocking agent). They were then exposed to 1.5, 15, or 150 ng/μL of biotinylated test GAG suspended in SMI buffer for 90 minutes at 4°C. The arrays were washed three times, 5 minutes per wash, with 5 mL SMI buffer at 4°C. Parallel negative (buffer alone) and positive (100 nM Alexa Fluor 647-conjugated staurosporine, known to bind one of the proteins in the protoarray) control arrays were run simultaneously. Arrays were exposed to 1 μg/mL Alexa Fluor 647-conjugated streptavidin in SMI for 30 minutes at 4°C. They were washed three times, 5 minutes per wash, in 5 mL SMI buffer at 4°C and then quickly rinsed in water before drying and scanning (Axon 4000B fluorescence scanner; Molecular Devices, Sunnyvale, CA). Data were acquired (GenePix Pro 6.0 software; Molecular Devises) and analyzed (ProtoArray Prospector software; Invitrogen).

Four criteria were used to define a significant interaction between a v4 protein and bGAGs: (1) A *Z*-score, or normalized fluorescence signal, greater than 3.0 SD above the mean human protein signal for nonreactive proteins in the test array, and a *Z*-score less than 1.0 in the negative control assay; (2) a *Z*-factor greater than 0.5, meaning that the signal was at least two times greater than the negative control; (3) a Cl $P < 0.05$, where the Cl *P*-value assigns a probability that the signal is derived from the distribution of signals arising from a set of defined negative controls; (4) a replicate spot CV less than 50%, where CV is the coefficient of variation for the assay from duplicate spots, determined by dividing the SD of the spot signals for all the spots by their mean spot intensity. A *Z*-score $> 3$ required a signal of ~15,600 RFU (relative fluorescent units) or greater to be classified as a positive binding protein for KS, and a signal of ~13,000 RFU or greater to be classified as a positive binding protein for CSA. For HA, there were only two proteins that met these stringent threshold criteria, and thus a *Z*-score $> 1$ was used to identify additional potential hits. The custom SEMA3A-Fc plate, probed with bKS at the same time as the KS-v4 protoarray, was scored based on the presence of signal that was significantly higher than the signal seen when the custom array was probed with detection reagent alone (result included as the final listing in Table 2).

To further investigate binding of corneal stromal GAGs to ECM nerve-related molecules, we purchased selected extracellular epitopes of growth factors, nerve growth cone guidance ligands, and their receptors from R&D Systems, and asked Invitrogen to create a custom nerve-related protein array and assay binding of bKS, bCSA, and bHA to these proteins using their standard protocol. The protein epitopes used in this custom array are shown in Table 1. To maximize their tertiary structure and biological activity, R&D Systems expresses many extracellular epitopes as fusion proteins with an added human IgG1 Pro100-lys330 domain (Accession # P01857). To assess whether GAGs react with this IgG1 epitope, or whether the fused IgG1 epitope might block the reaction of a GAG with a target protein, Invitrogen conducted a small test protoarray using bKS as the representative GAG, the IgG1 domain alone, NTR3, NTR3-Ig, EFNA1-Ig, and Semaphorin 3A-Ig. bKS reacted with NTR3-Ig, EFNA1-Ig, and SEMA3A-Ig, but not with IgG1 alone or with NTR3 from which the IgG1 domain had been cleaved. These results suggest that GAGs do not bind the IgG1 epitope, and that the presence of the IgG1 fusion domain does not block the reaction of a GAG with a target protein. For thoroughness, both the IgG1-tagged version and the IgG1-cleaved version for every protein for which both forms were available were included in the custom array. Each protein was spotted in duplicate from solutions of 10, 25, or 50 ng/μL in PB and bGAGs were used at 1.5, 15, or 150 ng/μL in SMI buffer. Proteins were scored as GAG binders if the difference between the RFU value measured on the negative control assay (buffer only) and the assay probed with the bGAG was greater than 2000 RFU for any concentration of the probe GAG.

## Mimecan Protoarray

The KS core protein mimecan was used by Invitrogen to probe its v4 protoarray, according to the same format as described for the GAG protoarrays, except that the test ligand was purified mouse mimecan, tested at 5 and 50 ng/μL. After incubation of the protoarray slides with mimecan, the slides were washed, incubated with rat anti-mouse mimecan, and then with Alexa-Fluor 647-labeled goat anti-rat IgG. For

the mimecan protoarray, the negative control was buffer alone, and the positive control was V5-his tagged yeast calmodulin kinase 1, developed with Alexa-Fluor 647-labeled anti-V5 antibody. The reaction of calmodulin kinase 1 with calmodulin protein in the v4 protoarray served as an indicator that the assay functioned properly. Data were acquired (GenePix Pro 6.0 software; Molecular Devices) and analyzed (ProtoArray Prospector software; Invitrogen) as for the GAG protoarrays. The criteria for a positive reaction between mimecan and a v4 protein were as described for the v4 bGAG assays.

### Surface Plasmon Resonance

SA sensor chips were conditioned with three consecutive 1-minute injections of 1 M NaCl in 50 mM NaOH before ligand was immobilized. bKS was dissolved in 0.01 M HEPES (pH 7.4), 0.15 N NaCl, and 0.005% (vol/vol) HSB-P buffer at 0.01 mg/mL and immobilized on flow cell (Fc) lanes 2 to 4 of an SA chip, using an injection time of 1 minute at a flow rate of 10 $\mu$L/min. A control of biotin alone was then immobilized on Fc lane 1 of each SA chip, with a saturated solution of biotin in HSB-P buffer under the same protocol. The four lanes of the chip were then washed with HSB-P buffer according to the manufacturer's protocol (GE/Biacore). Successful immobilization of biotinylated-KS was confirmed by a 290 to 300 RU increase (where one RU is equivalent to 1 pg protein/mm$^2$ on the sensor's surface) in the appropriate sensor chip lane. RU increase for the biotin lane was less than 50 RU. All data were blanked against the biotin control reference Fc (Fc1) and double-referenced against an HBS-P buffer injection (SLIT2 at 0 nM). Protein samples were diluted in HSB-P. Protein solutions were passed over the biotin-KS-coated sensor surface (KINJECT mode, model 3000; GE/Biocore) at a flow rate of 20 $\mu$L/min with a total injection volume of 100 $\mu$L, which flowed over the chip lanes sequentially from lane 1 to 4. After each run of a given protein concentration, dissociation was conducted in HSB-P buffer for 600 seconds, and regeneration of the sensor surface was conducted in 1 M NaCl in 50 mM NaOH. The response was monitored as a function of time (sensorgram) at 25°C, using automated in-line reference subtraction to subtract biotin control ligand binding in Fc1 from biotin-KS ligand binding in Fc2, 3, and 4. The kinetic parameters $k_a$ and $k_d$ (association and dissociation rate constants, respectively) were analyzed simultaneously using global fit. System software (BIAevaluation software ver 3.1; GE/BIAcore) simultaneously fitted the sensorgrams obtained at different concentrations of ligand, fixing each kinetic parameter to a single value for each set of experimental data. An apparent equilibrium dissociation constant ($K_D$) was calculated as the ratio $k_d/k_a$ with the maximum capacity ($R_{max}$) of the surface floated during the fitting procedure.

## Results

### KS, CSA, and HA Binding of Human Cellular Proteins

Bovine corneal KS binding to a very wide variety of proteins was assessed by Invitrogen with their v4 Protoarray, with more than 8000 human proteins or protein variations. A complete and searchable list of all v4 proteins, including an Invitrogen identification number, their location on v4 protoarray plates, an estimation of their concentration if they are GST-tagged proteins, and their exact amino acid sequence may be viewed at their website (http://hdl.handle.net/2097/1716). When screened at 150 ng/$\mu$L (10 $\mu$M), KS gave positive binding responses with 217 v4 proteins. With the exception of ABL1 homologue 1 variant a, each protein that KS bound is listed only once in Table 2, at the level of its highest binding, even when alternative forms or amounts of the protein, present in the different locations on the protoarray slides, also interacted with KS. An expanded version of Table 2, showing all proteins at all locations on the v4 protoarray slides that reacted with KS can be viewed at http://hdl.handle.net/2097/1716. Extracellular SEMA3A linked to $IgG_1$, obtained from R&D Systems, also was included in this analysis, and the response of 150 ng/$\mu$L bKS to 40 ng/$\mu$L SEMA3A-Fc is listed at the end of Table 2. The reproducibility of the KS-v4 protein binding results is supported in several ways: (1) The coefficient of variation of bKS binding to duplicate spots of a given protein at any one location in the v4 protoarray plates was never more than 12% for any positive KS-binding protein (see expanded Table 2 at http://hdl.handle.net/2097/1716); (2) binding of bKS to ABL1 homologue 1 variant a, occurred at all five duplicate locations of ABL1 homologue 1 variant a in the v4 protoarray in which the variation between the ABL1 homologue 1 variant a locations was only 1 amino acid, with very similar binding strengths of 43,459, 38,005, 36,821, 35,400, and 35,199 (Table 2). In contrast, bKS did not bind severely truncated versions of ABL1 homologue 1 variant a spotted at two other locations (see locations 2178 and 2878 in the total v4 proteins list at http://hdl.handle.net/2097/1716); and (3) 150 ng/$\mu$L bKS bound SEMA3A-Fc plated at 40 ng/$\mu$L in the first small custom protoarray shown at the end of Table 2 (5913 RFU) at a level very similar to its binding to SEMA3A-Fc plated at 50 ng/$\mu$L in the second larger custom protoarray shown in Table 5 (8203 RFU).

Nine of the 217 respondents were still positive when the screening was conducted at 15 ng/$\mu$L KS (ABL1, TBK1, PLK1, AXL1, NUAK1, CHUK, CCNT1, KCNAB2, and RPS6KA1), whereas only KCNAB2 was positive when the screening was conducted at 1.5 ng/$\mu$L KS. Of proteins that bound 150 ng/$\mu$L KS, 75 were protein kinases, comprising several families: (1) 10 cytoplasmic tyrosine kinases: ABL2, ABL1, BMX, BTK, PTK2B, SRC, FES, HCK, YES, and LYN; (2) 15 cytoplasmic domains of receptor tyrosine kinases: EPHA2, EPHA3, EPHA8, Ntrk1, Ntrk2, Ntrk3, wt KIT, two KIT point mutations, CSF1R, FGFR1, KDR, one FLT3 point mutation, ERBB2, and AXL; (3) four MAP kinase family members: MAP2K2, MAP2K6, one MAP2K6 point mutation, and MAP3K10; (4) four NIMA-related kinases: NEK1, NEK2, NEK3, and NEK4; (5) casein kinases epsilon 1, gamma 2, and gamma 3; (6) aurora kinases AURKA and AURKB; (7) death-associated protein kinases DAPK2, DAPK3; (8) ribosomal protein S6 kinases RPS6KB2, RPS6KA1, RPS6KA2, and RPS6KA4; (9) testis-specific serine kinases TSSK1B and TSSK2; (10) MAP/microtubule affinity regulating kinases MARK4 and MARK2; and (11) STE20-related kinases PAK1, STK24, and STK25. In addition, there were 13 membrane or secreted proteins that bound to 150 ng/$\mu$L KS: COL23A1, KCNAB2, ITGA6, CACNB1, EBAG9, SIRPG, PCDHGC3, SCYE1, F11R, CAPRIN1, ADD2, SYTL2, and BAIAP2. KS also bound 18 proteins involved in actin or microtubule binding or regulation: ABLIM1, CTNNA1, EPB39, LIMCH1, PAK4, ADD2, MAP2, AURKA, AURKB, DMN2, TPPP, MARK2, MARK4, MAPRE1, KIF2C, KIF3B, CTNNA1, and ACTR1B; and 20 proteins known or thought to be involved in nervous tissue function: Ntrk1, Ntrk2, Ntrk3, EPHA2, EPHA3, EPHA8, CAPRIN, BAIAP2, MAP2K10, SYTL2, DCX, HOMER2, TPPP, GSK3B, KCNAB2, MAP2, MARK4, PQBP1, ACTR1B, and extracellular SEMA3A.

In comparison, sturgeon notochord CSA bound only 23 v4 proteins when the screening was conducted at 150 ng/mL, listed in Table 3. Of these, seven (CSNK1A1, CHUK, PAK1, RPS6KA5, FLT1, MAP4K4, and GADD45GIP1) displayed their highest binding at a bCSA screening concentration of 15 ng/$\mu$L, whereas only three (PLK1, HADH, and NUDT16L1) were still positive when the screening was performed at 1.5 ng/$\mu$L. Of the CSA-binding proteins, 10 were kinases: 2 were independent preparations of PLK1, CHUK, PAK1, RPS6KA5, FLT1, MAP4K4, CSNK1D, and PAK4; 2 were nuclear proteins identified with the cell cycle or DNA or RNA binding: NUDT21 and GADD45GIP1; and 2 were cell surface or scaffold proteins:

**TABLE 3.** CSA Interaction with Invitrogen Proteins

| Protein | Signal | Accession No. | Invitrogen ID | Protein Description |
|---|---|---|---|---|
| PLK1 | 64,679 | NP_005021 | PV3501 | Polo-like kinase 1 (Drosophila) |
| ITGA6 | 62,823 | NP_000201.2 | NM_000210.1 | Integrin, alpha 6, transcript variant 2 |
| HADH | 61,418 | NP_005318.2 | BC000306.1 | Hydroxyacyl-Coenzyme A dehydrogenase |
| KCNAB1 | 60,955 | NP_751892.1 | NM_172160.1 | Potassium voltage-gated channel, shaker-related subfamily, beta 1 |
| NUDT16L1 | 60,163 | NP_115725.1 | NM_032349.1 | Nudix (nucleoside diphosphate linked moiety X)-type motif 16–1 |
| CSNK1A1 | 59,748 | NP_001883 | PV3850 | Casein kinase 1, alpha 1 |
| CHUK | 54,364 | NP_001269 | PV4310 | Conserved helix-loop-helix ubiquitous kinase |
| COASY | 47,848 | BC020985.1 | BC020965.1 | Coenzyme A synthase |
| KRTAP13-1 | 47,443 | NP_853630.2 | NM_181599.1 | Keratin associated protein 13–1 |
| PAK1 | 39,059 | NP_002567 | PV3820 | p21/Cdc42/Rac1-activated kinase 1 (STE20 homologue, yeast) |
| RPS6KA5 | 38,929 | NP_004746.2 | PV3681 | Ribosomal protein S6 kinase, 90kDa, polypeptide 5 |
| FLT1 | 37,750 | NP_002010 | PV3666 | Fms-related tyrosine kinase 1 receptor |
| MAP4K4 | 30,089 | NP_004825 | PV3687 | Mitogen-activated protein kinase kinase kinase kinase 4 |
| KIAAA0515 | 29,800 | BC012289.1 | BC012289.1 | KIAAA0515 |
| HOMER2 | 28,772 | NP_004830.2 | BC01209.1 | Homer homologue 2 (Drosophila) |
| GADD45GIP1 | 27,379 | NP_443082.2 | BC013039.1 | Growth arrest and DNA-damage-inducible gamma interacting prot. |
| CSNK1D | 26,494 | NP_620693 | PV3665 | Casein kinase 1, delta |
| SLAIN2 | 26,324 | NP_065897.1 | BC031691.2 | SLAIN motif family, member 2 |
| C11orf66 | 25,433 | NP_659454.1 | BC053995.1 | Chromosome 11, open reading frame 66 |
| ACOX1 | 24,045 | NP_004026.2 | BC010425.1 | Acyl-coenzyme A oxidase 1, palmitoyl |
| PAK4 | 23,005 | NP_005875.1 | NM_005884.2 | p21(CDKN1A)-activated kinase 4 |
| NUDT21 | 22,423 | NP_008937.1 | NM_007006.1 | Nudix (nucleoside diphosphate linked moietyX)-type motif 21 |
| PLK1 | 19,806 | NP_005021 | NM_005030.2 | Polo-like kinase 1 (Drosophila) |

$n$ = 23 of 8,268 proteins screened.

ITGA6 and HOMER2. Again, reproducibility of bCSA binding in this proteomics protocol is supported in several ways. (1) The coefficient of variation between adjacent duplicate protein spots never exceeded 16% (data not shown). (2) PLK1 was spotted in four different duplicate locations in the v4 protoarray. One duplicate PLK1 version at one location was the highest binder of bCSA (64679RFU; Table 3) and had a His-tag instead of the usual GST tag on most v4 proteins, which caused it to be printed at a higher concentration than GST-tagged proteins. A second PLK1 duplicate spot location was the lowest reported binder of bCSA (19806RFU; Table 3), and was plated at a lower concentration than was retained at the highest binding location. PLK1s at a third and fourth location were plated at concentrations one fourth that of the concentration at the second location, the version at the fourth location was severely truncated, and neither location gave a positive signal for bCSA binding. These results demonstrate a concentration dependency for CSA-protein binding.

In contrast, chicken cockscomb HA bound only six of the >8000 v4 proteins (Table 4). Of these six proteins, three (KRTAP13–1, IRS1, and HADH) achieved their highest binding at an HA screening concentration of 150 ng/$\mu$L, one (LGALS8) showed its highest binding at an HA screening concentration of 15 ng/$\mu$L, and two (GFAP and CABP4) displayed their highest binding at an HA screening concentration of 1.5 ng/$\mu$L. Overall, the signal intensity for all three bHA screenings was low compared with the signal intensities for bKS and bCSA screenings, with only KRTAP13-1 generating a signal intensity above the lowest positive v4 intensities obtained with bKS and bCSA. Again, the coefficient of variation between adjacent duplicate spots was never higher than 16% (data not shown), suggesting good binding reproducibility for bHA. In addition, although only one of the six v4 proteins bound by bHA was present more than once in the v4 protoarray, a complete version of galectin 8 (LGALS8) and a variant version lacking an internal segment of the protein and plated at approximately one tenth the concentration of the complete version, bHA bound the more concentrated complete version at a level significantly above background noise, but did not bind the much less concentrated variant lacking the internal segment. Whereas these results could reflect either the avidity of HA for LGALS8 or the ability of HA to discriminate between full length and internally truncated LGALS8, they suggest that the protoarray protocol used in our experiments allowed bHA to bind protein spots discriminately.

**TABLE 4.** HA Interaction with Invitrogen Proteins

| Protein | Signal | Accession No. | Invitrogen ID | Protein Description |
|---|---|---|---|---|
| KRTAP13-1 | 38,193 | NP_853630.2 | NM_181599.1 | Keratin-associated protein 13-1 |
| IRS1 | 14,035 | NP_005535.1 | BC053895.1 | Insulin receptor substrate 1 |
| GFAP | 4,593 | NP_002046.1 | NM_002055.1 | Glial fibrillary acidic protein |
| HADH | 4,296 | NP_005318.2 | BC000306.1 | Hydroxyacyl-coenzyme A dehydrogenase |
| LGALS8 | 2,944 | NP_006490.3 | BC015818.1 | Lectin, galactoside-binding, soluble, 8 (galectin 8) |
| CABP4 | 2,443 | NP_660201.1 | BC033167.1 | Calcium binding protein 4 |

$n$ = 6 of 8268 proteins screened.

**Table 5.** KS Interaction with Nerve-Related Extracellular Molecules and Epitopes

| Protein | Signal | Accession No. | Protein Description |
|---|---|---|---|
| SLIT3 | 41,488 | Q9WVB4 | Mus Ser27-His901; secreted axon guidance factor; Robo ligand. |
| DCC-Fc | 39,177 | NP_031857 | Deleted in colorectal carcinoma, Mus Met1-Asn1097 + LINK + HumIgG Pro100-Lys 330; attractive response toward netrin-1. |
| ERBB4 | 33,716 | Q15303 | Hum Glu26-Arg649. Type 1 glycoprotein, Tyr protein kinase, and epidermal growth factor receptor. |
| SEMA3F-Fc | 26,174 | QO88632 | Mus Ala19-Pro775 + link + HumIgG Pro100-Lys 330. Secreted, sema domain, Ig domain, short basic domain, neuroguidance. |
| ERBB2-Fc | 25,936 | NP_004439 | Hum Thr23-Thr652 + Link + HumIgG Pro100-Lys 330. Type 1 glycopro, Tyr protein kinase and epidermal growth factor receptor. |
| EFNA3-Fc | 19,524 | NP_004943.1 | Ephrin A3 extracellular domain Hum(aa 1–209) + link + HumIgG Pro100-Lys 330; binds Eph receptors in developing neural tissue. |
| ROBO1-Fc | 19,284 | 055005 | Hum Met1-Ala16 + rat Lys 19-Lle 560+link+HumIgG Pro100-Lys 330. Neural tissue negative Slit receptor. |
| EFNA1-Fc | 16,592 | P52793 | Ephrin A1: Mus Asp19-Ser182 + link + HumIgG Prb100-Lys 330. Binds Eph receptors in developing neural tissue. |
| EFNB3-Fc | 16,459 | NP_001397.1 | Ephrin B3: Hum Met1-Ser224 + Link + HumIgG Pro100-Lys 330. Binds Eph receptors in developing neural tissue. |
| EFNB1-Fc | 14,809 | Q544L9 | EphrinB1: Mus Lys30-Ser229 + Link + HumIgG Pro100-Lys 330. Binds Eph receptors in developing neural tissue. |
| EFNB2-Fc | 13,578 | AAA82934 | Ephrin B2: Mus Arg27-Ala227 + Link + HumIgG Pro100-Lys 330. Binds Eph receptors in developing neural and angiogenic tissue. |
| EPHB4-Fc | 13,620 | P54760 | Ephrin B4: Mus Leu16-Ala539. Tyr kinase receptor, binds EFNB2. Inhibits cell-cell adhesion and angiogenesis. |
| SEMA6A-Fc | 12,914 | NP_065847.1 | Semaphorin 6A: Hum Met1-Thr649 + Link + HumIgG Pro100-Lys 330. Anchored transmembrane signaling molecule. Negative axon guidance. |
| EPHA1-Fc | 12,040 | NP_005223.4 | Ephrin A1: Hum Met1-Glu547 + Link + HumIgG Pro100-Lys 330. Tyr receptor kinase. Binds EFNA1 in neuronal and angiogenic tissue. |
| EPHB3-Fc | 10,730 | NP_034273.1 | EphB3: Mus Met1-Thr530 + Link + HumIgG Pro100-Lys 330. Transmembrane Tyr kinase receptor; binds EFNB1, -B2, -B3. |
| ROB02-Fc | 10,188 | NP_002933.1 | Hum Met1-Ala312 + Link + Hum ROB02 Pro313-Pro859 + HumIgG Pro100-Lys 330. Neural tissue negative Slit receptor; permissive of neurite outgrowth via ROB01-ROB02 interaction. |
| SEMA3E | 10,117 | 0150041 | Semaphorin 3E: Mus Thr25-Ser775(Arg557Alaand Arg560A1a) secreted, axon and vascular tip cell chemorepellant; binds plexin. |
| ERBB4-Fc | 9,140 | Q15303 | HumGlu26-Arg649 + Link + HumIgG Pro100-Lys 330. Type I glycoprotein, tyr kinase and epidermal growth factor receptor. |
| SEMA3A-Fc | 8,203 | Q14563 | Semaphorin3A: Hum Lys26-Val771 + link + HumIgG Pro100-Lys 330. Secreted, binds nerve cell Neuropilin1+PlexinA receptor complex; neurorepellant. |
| EFNA2-Fc | 8,113 | NP_031935.3 | Mus Met1-Asn184 + Link + HumIgG Pro100-Lys 330. Binds EPH A2, -A3, -A4, -A5, -A6, -A7, -A8 receptors. Fens in neuroguidance and angiogenesis. |
| Ntrk3-Fc | 7,250 | NP_002521 | Neurotrophic tyrosine kinase, type 3; binds secreted NT-3. |
| EPHA8-Fc | 7210 | NP_031965.2 | Ephrin A8 Mus Met1-Arg540 + Link + HumIgG Pro100-Lys 330. Transmembrane Tyr kinase receptor; binds EFNA5, -A3,-A3. |
| SEMA6A | 7,110 | NP_065847.1 | Semaphorin 6A: Hum Met1-Thr649. Anchored transmembrane signalling molecule. Negative axon guidance. |
| NTN1 | 6,956 | AAC52971 | Netrin1: Mus Va122-Ala603. Secreted neuroguidance molecule; interacts with DCC, UNC5 family, and neogenin receptors. |
| NRG1 | 6,607 | NP_039253.1 | Human neuregulin1, SMDF isoform, lacks Ig-like domain, Transmembrane domain, and cytoplasmic tail. Secreted neuroattractant. |
| SEMA6B-Fc | 6,607 | Q9H3T3 | Semaphorin 6B: Hum CD33Met1-Ala16 + Hum Sem6B Leu26-Ser603 + Link + HumIgG Pro100-Lys 330. Type I glycoprotein with semaphorin domain. Binds Plexin4 w/o neuropilin1; axon repulsion. |
| EFNA5-Fc | 6,397 | NP_001953.1 | Ephrin A5: Hum Met1-Asn203 + Link + HumIgG Pro100-Lys 330. Binds EPHsSA2-A8. Neurorepellant in neural tissue. |
| UNC5H2-Fc | 5,989 | NP_071543.1 | Rat Met1-Asp373 + Link + HumIgG Pro100-Lys 330. Transmembrane NTN receptor that mediates neurorepulsion with NTN1. |
| EPHA6-Fc | 5,886 | NP_031964.2 | Ephrin A6: Mus Met1-Gln546 + Link + HumIgG Pro100-Lys 330. Transmembrane EFN receptor. |
| NGFR-Fc | 5,833 | NP_001057.1 | Low affinity nerve growth factor receptor: Hum p75 Met1-Asn250 + Link + HumIgG Pro100-Lys 330. Binds NGF, NT3, NT4. |
| PDGFAB | 5,617 | NP_036933.1<br>NP_113712.1 | Dimerized rat PDGFA Ser87-Aug196 and rat PDGFB Ser74-Thr182. Binds to receptor kinases PDGF-$\alpha$ and PDGF-$\beta$. |
| EFNA4-Fc | 5,590 | NP_031936.2 | Ephrin A4: Mus Met1-Gly176 + Link + HumIgG Pro100-Lys 330. Binds EPHA2-A7, -B1. Important in neurogenesis and angiogenesis. |
| EPHA7-Fc | 5,435 | NP_001116361.1 | Ephrin A7: Mus Met1-Pro549 + Link + HumIgG Pro100-Lys 330. Tyrosine kinase receptor for EFNA1-A5. Neurogenesis and angiogenesis |
| NTN2 | 4,894 | Q90923 | Netrin 2: chicken CD33 Met1-Met17 + chicken NTN2 Ala16-Pro 581. Secreted neuroguidance molecule; interacts with DCC, UNC5 family, and neogenin receptors. |

(*continues*)

**TABLE 5** (*continued*). KS Interaction with Nerve-Related Extracellular Molecules and Epitopes

| Protein | Signal | Accession No. | Protein Description |
|---|---|---|---|
| NTN4 | 4,785 | AAG53651 | Netrin 4: Hum Met1-Lys628. Secreted neuroguidance molecule; interacts with DCC, UNC5 family, and neogenin receptors. |
| EPHB1-Fc | 4,184 | XP_001081949.1 | EPHB1: Hum CD33 Met1-Ala16 + Rat EPHB1 Met18-Gln538 + Link+HumIgG Pro100-Lys 330.Binds EFNA1, -A3, -A4, -B1, -B2, -B3. |
| EPHA3-Fc | 3,279 | NP_034270.1 | Ephrin A3: Mus Met1-His541 + Link + HumIgG Pro100-Lys 330. Binds EFNA1–A5, -B1. |
| EPHA4-Fc | 3,014 | NP_031962.2 | Ephrin A4: Mus Met1-Thr547 + Link + HumIgG Pro100-Lys 330. Binds EFNA1–A5, -B2, -B3. |
| SEMA4A-Fc | 2,996 | NP_071762.2 | Semaphorin 4A: Hum Gly32-His 683 + Link + HumIgG Pro100-Lys 330. Transmembrane; fcns in immune and nervous tissue. |
| SEMA3F | 2,377 | O88632 | Semaphorins F: Mus A1a19-Pro775(arg583A1a and Arg586A1a). Secreted, interacts with plexinA3 and neuropilin2, chemorepellant. |

$n$ = 40 of 85 proteins screened. EFN A, GPI-membrane-anchored; EFN B transmembrane. Only membrane-bound or Fc-clustered ligands (Ephrins) can activate EPHs.

## KS, CSA, and HA Binding of Extracellular Epitopes of Nerve-Related Proteins

The anterior cornea is one of the most highly innervated tissues on the surface of the human body.[57] Because KS, CSA, and HA are present in very high concentrations in the corneal ECM, we asked whether these GAGs bind some of the neuroregulatory molecules or epitopes of membrane-bound neuroregulatory molecules whose mRNAs are known to be expressed in the developing cornea.[53] Because of our previous localization of SLIT2 mRNA in the anterior cornea and the high amino acid sequence homology between SLIT orthologues,[58] we included SLIT3 in our custom array, because it was the only SLIT orthologue R&D Systems had available at the time.

Bovine corneal bKS bound 44 of the 85 nerve-related proteins or protein epitopes for the nerve-related custom protoarray analysis, listed in Table 5. In addition to the high similarity of bKS binding to SEMA3A-FC shown in both the first and the second custom array experiments, reproducibility of bKS nerve-related protein binding is supported by its concentration dependency. For the nerve-related protein custom arrays, all proteins were plated in duplicate spots at three or four separate locations at different concentrations and screened with three different GAG concentrations. For many KS interactant proteins, there was a concentration-dependent increase in RFU signal, with increasing signals being observed both with higher KS concentrations and at spots corresponding to higher concentrations of protein on the arrays (data not shown).

In agreement with the results of preliminary tests (see the Methods section), in 20 of the 29 sets of $IgG_1$-tagged/cleaved target protein epitopes, bKS bound the $IgG_1$-tagged version of the protein, but not the $IgG_1$-cleaved version. In two additional cases (SEMA3F and SEMA6A), KS bound the $IgG_1$-tagged version better than the $IgG_1$-cleaved version; in one case (ERBB4), KS bound the $IgG_1$-cleaved version better than the $IgG_1$-tagged version; and in six cases, KS bound neither version (Ntrk1, EPHA2, EPHA5, EPHB2, EPHB6, and NRP2).

Of the 85 nerve-related epitopes in the protoarray, bKS bound most strongly the neuroregulatory ligand SLIT3; KS also bound the extracellular epitopes of SLIT receptors ROBO1 and -2. The second and third most strongly bound epitopes were deleted in colorectal carcinoma (DCC), a netrin receptor, and ERBB4, a neuregulin receptor. KS bound all the neuroguidance SEMA epitopes in the protoarray, but did not bind either of the SEMA receptor epitopes, neuropilin-1 or -2 (NRP1 or -2). There were no NRP coreceptor plexin epitopes available for the nerve-related protoarray. In the EFN/EPH neuroguidance family, KS bound the extracellular epitopes of all the EFN ligand epitopes in the protoarray, but only 9 of 13 EPH receptor epitopes in the protoarray. In the NTN/DCC/UNC5H family, KS bound all the NTN-soluble ligand epitopes in the array, the one DCC receptor epitope in the array, and one of the four uncoordinated 5H (UNC5H)-negative NTN receptor epitopes in the array. In the neuroattractant NT/Ntrk family, KS did not bind the soluble NT-3 neuroattractant ligand, but did bind the NT3-specific Ntrk3 receptor epitope and the less NT isoform-specific NGFR receptor. KS did not bind the other two NT receptors, Ntrk1 and -2. In the Schwann cell–regulating NRG/ERBB family, KS bound both the soluble NRG1 SMDF Schwann cell attractant/stimulatory ligand and the two SMDF ERBB receptor epitopes that were in the protoarray. Of the other soluble growth factors in the protoarray, KS bound PDGF, but did not bind EGF, acidic or basic FGF, or TGF$\beta$1. Finally, KS did not bind either of the assembled integrin epitopes in the protoarray, integrin alpha V beta 3 ($\alpha V\beta 3$), or integrin alpha 3 beta 1 ($\alpha 3\beta 1$).

In comparison, sturgeon notochord CSA bound only 9 of the 85 nerve-related proteins or protein epitopes in the nerve-related protoarray (Table 6). Secreted neuroguidance ligand NTN4 and one of its UNC5H negative receptor epitopes were the strongest CSA binders, whereas the DCC-positive receptor epitope bound less strongly, and the other NTN and UNC5H isoforms in the protoarray were not bound by CSA. Two neuroregulatory SEMA isoform epitope ligands were slightly bound, along with two EFN ligands, one EFN receptor EPH epitope isoform, and one SLIT neuroguidance receptor ROBO epitope isoform. Of the 29 epitopes that were present in the protoarray in both the $IgG_1$-tagged and $IgG_1$-cleaved forms, CSA bound 5, and in each case it bound the tagged version, but not the cleaved version. Binding strengths for nerve-related CSA binders were significantly lower than were binding strengths for KS binders (compare Table 6 to Table 5).

bHA did not bind any proteins in the nerve-related extracellular epitope protoarray.

## KS Core Protein Mimecan Interactions with v4 Proteins

The KS core protein mimecan (OGN) bound 15 of the 8000+ proteins in the v4 array, listed in Table 7. Of these 15 proteins, mimecan bound SLAIN2, a ubiquitously expressed $\beta$-tubulin-like protein of unknown function that is widely conserved in vertebrates,[59] with a higher signal than any signal generated by bKS, bCSA, or bHA binding to any protein. The next highest binder, UBXD3, generated one fifth the signal intensity, and the other 13 binders gave signal intensities below one fifth the mimecan-SLAIN2 intensity. Mimecan binders included two members of the casein kinase 1 family: delta and epsilon; two different potassium channel proteins: KCNAB1 and KCNAB2; and three kinases that have roles in microtubule formation or stabilization: MARK2, AURKA, and PLK1.

**Table 6.** CSA Interaction with Extracellular Nerve-Related Molecules and Epitopes

| Protein | Signal | Database ID | Protein Description |
|---|---|---|---|
| NTN4 | 7,468 | AAG53651 | Netrin 4: Hum Met1-Lys628. Secreted neuroguidance molecule. |
| UNC5H1-Fc | 4,515 | NP_071542.1 | Uncoordinated: Hum CD33 Met1-Ala16 + Rat UNC5H1 Gln26-Asp358). Receptor for secreted NTN axon guidance ligands. |
| SEMA6B-Fc | 4,264 | Q9H3T3 | Semaphorin 6B: Hum CD33Met1-Ala16 + Hum Sem6B Leu26-Ser603 + Link + HumIgG Pro100-Lys 330. Transmembrane glycoprotein that fens in neuroguidance. |
| EFNA3-Fc | 4,144 | NP_004943.1 | Ephrin A3 extracellular domain Hum(aa 1–209) + link + HumIgG Pro100-Lys 330; binds Eph receptors in developing neural tissue. |
| EPHA1-Fc | 3,062 | P52793 | Ephrin A1: Mus Asp19-Ser182 + link + HumIgG Pro100-Lys 330. Binds Eph receptors in developing neural tissue. |
| DCC-Fc | 2,933 | NP_031857 | Deleted in colorectal carcinoma, Mus Met1-Asn1097 + LINK + HumIgG Pro100-Lys 330; attractive response toward netrin-1. |
| SEMA3E | 2,591 | 0150041 | Semaphorin 3E: Mus Thr25-Ser775 (Arg557Alaand Arg560Ala) secreted, axon and vascular tip cell chemorepellant; binds plexin. |
| ROB02-Fc | 2,546 | NP_002933.1 | Hum Met1-Ala312 + Link + Hum ROB02 Pro313-Pro859 + HumIgG Pro100-Lys 330. Neural tissue negative Slit receptor. |
| EPHB2-Fc | 2,442 | P29323 | Ephrin B2: Hum Met1-Leu543 + Link + HumIgG Pro100-Lys 330. Transmembrane receptor; interacts with EFNA5 and EFNB ligands. |

$n = 9$ of 85 proteins screened.

### Kinetic Studies of KS Interaction with SLIT2 as Determined by SPR

Our protoarray study revealed SLIT3 to be one of the most avid binders to KS. After the nerve-related protoarray had been completed, R&D Systems made SLIT2 available. Because SLIT2 mRNA is expressed in the anterior cornea[54] and has been shown to influence nerve growth cone migration differently, depending on whether it is bound by ECM molecules,[60,61] we characterized the interaction of KS with SLIT2 in more detail, performing SPR, with bKS immobilized on streptavidin-coated sensor chips. The kinetic analyses were performed by injecting SLIT2 at various concentrations over immobilized KS. As revealed by a typical sensorgram shown in Figure 1, binding of SLIT2 to KS was concentration dependent. For the analyses shown in Figure 1, the SLIT2 injection volume was 50 $\mu$L. Kinetic analyses for each SLIT2 concentration were performed in triplicate. As shown in Figure 2, SLIT2 binds to KS in a saturable manner, as evidenced by the logarithmic trend line. Kinetic data were fitted to a 1:1 Langmuir binding model (Table 8), allowing the calculation of the $k_a$ (kinetic association rate constant), the $k_d$ (kinetic dissociation rate constant), and the $K_D$ (apparent equilibrium dissociation constant). The $K_D$ for SLIT2 binding to KS was 28 nM, suggesting that KS binds SLIT2 with relatively high affinity.

By protoarray analysis, KS bound SEMA3A much less strongly than SLIT3, but binding was still significantly above background (Tables 2, 5). Repeated attempts to detect SEMA3A binding to immobilized KS using SPR were unsuccessful, using SEMA3A concentrations as high as 2 $\mu$M or 250 ng/$\mu$L.

## Discussion

In both the v4 protoarray and a custom extracellular nerve-related protoarray, corneal KS bound the greatest number of proteins. In contrast, sturgeon notochord CSA bound significantly fewer v4 proteins and extracellular nerve-related proteins than did KS. Nonsulfated cockscomb HA bound the fewest v4 proteins in comparison to corneal KS and sturgeon notochord CSA, and no extracellular nerve-related proteins at all. Mimecan, included in this study because it is the KS core protein about which the least protein-binding information is known, bound slightly more v4 proteins than did sturgeon notochord CSA and was not tested with our custom extracellular nerve-related protein array. However, binding strengths of 9 of the 23 sturgeon notochord CSA-binding candidates were higher than the binding strength of the strongest corneal KS-binding candidate. In contrast, binding strengths of five of the six nonsulfated HA-binders were lower than the strengths of any positive highly sulfated corneal KS- or highly sulfated CSA-binding proteins. Both corneal KS and sturgeon notochord CSA bound preferentially with the biologically active ($IgG_1$-tagged) form of almost all extracellular nerve-related epitope pairs, suggesting that the GAG-protein interactions observed in this study have potential in vivo relevance. Although generally regarded as extracellular, KS[24,62–66] and HA[50,51] have also been detected intracellularly. These GAG–protein binding profiles demonstrate that GAGs found in the corneal stroma may interact with many proteins, both intracellularly and extracellularly, and thus could influence the availability and/or the configuration of these proteins for subsequent interaction with their target cellular ligands/receptors.

Our study is the first to examine binding of corneal KS, sturgeon notochord CSA, or nonsulfated HA to a wide variety of cellular and ECM proteins using high-throughput protoarray techniques with the proteins immobilized on a fixed surface and the GAGs free in solution. Other protoarray studies examining GAG–protein interactions have immobilized naturally occurring and synthetic GAGs on a fixed surface and probed them with solutions containing a limited number of known proteins.[67,68] That the protoarray format can reveal new protein–GAG interactions is substantiated by the fact that in a study by Wang et al.[68] dermatan sulfate GAG was found to bind to an antibody not previously thought to bind it. In our study the protoarray format first revealed KS binding to a SLIT family member, which was then further defined for KS binding to SLIT2 by SPR studies. It is not clear from our and other comparative protein-GAG interaction studies whether it is better to attach the GAG or the protein to the fixed matrix, and what is optimal may differ for different GAGs and different proteins. Attaching some GAGs[69] and proteins[70] to a matrix has been found to impose structural constraints that have diminished their binding to some proteins. Also, some GAGs[67,71] and some

**TABLE 7.** Mimecan Interaction with Invitrogen v4 Proteins

| Protein | Signal | Accession No. | Invitrogen ID | Protein Description |
|---|---|---|---|---|
| SLAIN2 | 50,042 | NP_065897.1 | BC031691.2 | SLAIN motif family, member 2 |
| UBXD3 | 12,008 | NP_689589.1 | NM_152376.2 | UBX domain protein 3 |
| DYRK3 | 9,363 | NP_003573 | PV3837 | Dual specificity serine/threonine and tyrosine kinase 3 |
| APEX2 | 8,757 | NP_055296.2 | NM_014481.2 | Apurinic/apyrimidinic endonuclease 2, nuclear gene for mito protein |
| MARK2 | 8,389 | NP_059672.2 | PV3878 | MAP/microtubule affinity-regulating kinase 2 |
| CSNK1D | 7,668 | NP_620693 | PV3665 | Casein kinase 1, delta (serine/threonine kinase) |
| AURKA | 7,657 | NP_940839 | PV3612 | Aurora kinase A, serine/threonine, assoc. w centrosomes |
| KCNAB1 | 7,601 | NP_751891.1 | NM_172159.2 | Potassium voltage-gated channel, shaker-related, beta 1 |
| STK40 | 6,187 | NP_114406.1 | NM_03217.1 | Serine/threonine kinase 40 |
| C11orf63 | 5,318 | NP_954575.1 | NM_199124.1 | Chromosome 11 ORF 63, variant 2 |
| PLK1 | 4,143 | NP_005021 | PV3501 | Polo-like kinase 1 (Drosophila) associated with cell mitosis |
| TCP10L | 3,902 | NP_653260.1 | NM_144659.1 | t-Complex 10 (mouse)-like |
| KCNAB2 | 3,808 | NP_003627.1 | NM_003636.1 | Potassium voltage-gated channel, shaker-related subfamily, beta 2 |
| CENK1E | 3,308 | NP_001885 | PV3500 | Casein kinase 1, epsilon, association with DNA damage repair and cytokine |
| PAK6 | 2,995 | NP_064553 | PV3502 | p21(CDKN1A)-activated kinase 6, in testis and prostate |

$n$ = 15 of 8,268 screened.

proteins may attach better to a given matrix than others. In our study, HA in solution did not bind the known HA-binders aggrecan, link protein, and fibronectin affixed to a matrix, but it has been shown to bind link module when HA is the fixed moiety.[45,72] In our study, KS in solution bound SEMA3A in the protoarray format where SEM3A was the fixed moiety, but not in the SPR format where KS was the fixed moiety.

Although there are several indicators of reproducibility for the protein binders for KS, CSA, and HA detected in our protoarray protocol, our protocol failed to detect binding of some of these GAGs to proteins they have been reported to bind in other studies, such that these known GAG binders did not serve as positive controls in our protoarray study. The most probable reason that the v4 versions of aggrecan, link protein, or fibronectin did not serve as positive controls for HA binding in our proteomics study is that the v4 versions of these proteins are produced in insect cells and are therefore not glycosylated in the ways that these molecules are when produced under their usual human cell biosynthetic conditions. Deglycosylated aggrecan cannot bind HA,[73] and it is likely that the same is true for nonglycosylated link protein. In addition, fibronectin binding of HA requires that the fibronectin be both glycosylated and aggregated, and nonaggregated fibronectin bound to an affinity column does not bind HA.[74] In the same vein, although KS had been shown to bind IGFBP2 before this proteomics study, IGFBP2 could not serve as a positive control for KS binding in our proteomics screening format because IGFBP2 binds GAGs only if IGF-I or -II are present.[75] These considerations suggest that the proteins identified as GAG binders in our protoarray format bind those GAGs without being posttranslationally glycosylated or the participation of additional cofactors.

In many GAG-protein interaction studies, biotinylation is a common method of labeling either the proteins or the GAGs. In some protoarray studies, soluble protein ligands are labeled with biotin for detection after GAG binding.[67,68] We used immobilized proteins with solubilized bGAGs for detection. Others have also used bGAGs to study GAG interactions with immobilized proteins.[71–72,75–78] However, biotinylation procedures can biotinylate different positions within a GAG,[69] as occurred in our study with biotinylation of KS at only one end of its chain and biotinylation of CSA and HA all along their GAG backbones. In addition, biotinylation can have different efficiencies with different GAGs, again as it did in our study. These differences in biotinylation may have different effects on the functional properties of GAGs.[69,71,79] Similar position, efficiency, and steric hindrance effects may perturb the binding properties of proteins if they are the biotinylated moieties in GAG–protein binding studies. Also, many GAG–protein interaction studies using column chromatography or SPR protocols use the biotin of the bGAG to attach the GAG to the fixed substrate,[32,69,80] as we did in our SPR experiments. This method could magnify structural aberrations in a GAG to a

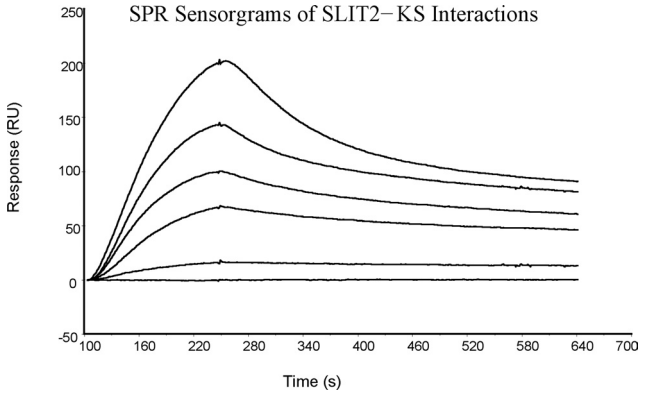


**FIGURE 1.** SPR sensorgrams of SLIT2-KS interactions. *Top* to *bottom*: concentrations of SLIT2 were 150, 130, 70, 50, 20, and 10 nM, respectively.

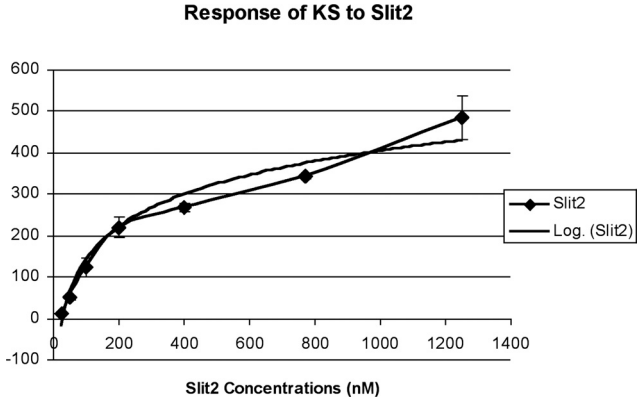


**FIGURE 2.** SLIT2 binds to KS in a concentration-dependent and saturable manner with a logarithmic trend line.

**Table 8.** Langmuir 1:1 Binding Model Data for Interaction between SLIT2 and Biotinylated KS

| | Keratan Sulfate |
|---|---|
| $k_a \times 10^3$, $M^{-1}$ | 1.17 ± 0.24 |
| $k_d \times 10^{-7}$, $s^{-1}$ | 3.45 ± 2.37 |
| $K_D$, nM | 27.77 ± 15.35 |

$k_a$, kinetic association rate constant; $k_d$, kinetic dissociation rate constant; $K_D$, apparent equilibrium dissociation constant.

greater or lesser extent, depending on where the GAG is biotinylated. Thus, protoarray techniques can suggest false GAG–protein interactions, and proteins identified by protoarray studies as GAG–binding proteins should be considered candidate GAG–binders until additional techniques confirm the GAG-protein binding.

GAGs are defined by their primary disaccharide structure, and therefore KS, CS, and HA have the same primary structure from one species to another. However, the extent and positions of sulfation of GAG disaccharides can vary considerably for any one kind of GAG, both from species to species, and also from tissue to tissue within a given species. Bovine and human corneal KS chains have similar charge densities and chain lengths, and the three most prevalent capping structures at the nonreducing termini are identical in relative proportions.[81] Therefore, it is likely that human corneal KS chains would bind v4 human proteins in a manner very similar to that displayed by bovine corneal KS. In contrast, sturgeon notochord CSA is 100% sulfated[82] (every disaccharide is monosulfated at C-4 of GalNAc), which is a higher percentage of disaccharide sulfation than is found in most human[83] or bovine[82] corneal CSA. The extent and positions of sulfate groups within CS chains have been shown to significantly affect CS binding to protein targets,[33,34,84] leading to the proposal of a sulfation code[85] for GAGs that governs their ability to interact with proteins. It is not known whether human corneal CSA chains may be asymmetrically sulfated, such that they have regions of high (100%) disaccharide sulfation contiguous with regions of low disaccharide sulfation. If they do, 100% sulfated regions (sulfation hot spots) of such human corneal CSA would be expected to show protein interactions similar to those seen with sturgeon notochord CSA, whereas the low sulfated regions may bind very different proteins. HA is never sulfated, so HA from any species or tissue should be equivalent in its binding properties with human proteins, as long as their average chain lengths are similar.

In our GAG protoarray studies, Invitrogen optimized conditions for KS binding in their protoarray protocol and then used the same general conditions for CSA and HA binding. It is possible that under other binding conditions, highly (or asymmetrically) sulfated CSA and/or HA would react with more candidate proteins. Alternatively, spotting complete posttranslationally modified forms of proteins such as aggrecan, link protein, or fibronectin on microarray plates may also increase the number and kinds of proteins that bind GAGs in a protoarray format. No mimecan binding proteins were known before our study, so it is difficult to assess whether the binding conditions used in this study were optimal for mimecan.

Because corneal KS, sturgeon notochord CSA, and HA are large linear polyanionic molecules, it is probable that electrostatic interactions are part of the mechanism involved in the protein-KS, -CSA, and -HA binding observed in our protoarray studies, as has been demonstrated in many heparin- and heparan sulfate-protein interactions.[86] Recent studies of reactions of yeast[87] and human[88,89] protein arrays with a range of biotinylated linear polyanionic macromolecules (actin, tubulin, heparin, heparan sulfate, and DNA) have defined a wide array of polyanionic binding proteins (PABPs), with sulfated GAGs binding the greatest number of different PABPs in each study. In addition, lack of reduction in the number of PABPs bound by increasing binding solution salt concentrations suggests that there are also noncoulumbic (e.g., hydrophobic and hydrogen binding) molecular interactions involved in protein-GAG binding.[88,89] Moreover, reacting proteins did not need to be positively charged overall, nor to have a specific GAG-binding signature sequence motif,[18] but only needed to have some positive subdomain along their amino acid sequence to be capable of polyanionic binding.[86–89] The authors argue that many proteins contain subdomains of amino acids that are probably unfolded in solution[90] and that these disordered regions may allow them to interact with many different binding partners with various degrees of strength or specificity by mechanisms such as electrostatic interaction that do not require tertiary structure complementarity. Similar considerations also apply to interactions of proteins like kinases with smaller anionic molecules such as single nucleotides.[89] In our study, 75 of the 217 KS-candidate v4 protein binders and 9 of the 23 CSA-candidate v4 protein binders were kinases. The catalytic domains of all kinases contain two invariant lysines and an arginine, with the serine/threonine kinases containing an additional invariant lysine, and the tyrosine kinases containing additional histidine, arginine, and lysine residues,[91] suggesting that kinase catalytic domains may have an overall basic charge that would allow them to interact electrostatically with polyanionic GAGs. Viewed more broadly, 28 of the top 50 KS-candidate binders and 11 of the 23 CSA-candidate binders could be classified as PABPs on the basis of their known binding to actin, microtubules, DNA, RNA, nucleotides, or nucleosides. HA's top protein interactants could also be viewed as potential PABPs. Keratin-associated protein 13-1 (KRTAP13-1), contains one partial (-RPR-) basic amino-acid–rich GAG-binding motif[18] in its short sequence.[92] Insulin receptor substrate 1 (IRS1), possesses numerous basic amino-acid–rich segments in its primary amino acid sequence and two ATP-binding sites.[93,94]

The nature of the interactions between mimecan and its 15 candidate v4 protein binding partners remains unresolved. The revelation that mimecan binds SLAIN2, a β-tubulin-like protein, and three kinases that regulate microtubule behavior suggests a possible role for mimecan in microtubule function in vivo. It is probable that the protein-binding behavior of mimecan core protein is altered when it is glycosylated with KS chains. Although all three corneal KS core proteins are small leucine-rich repeat proteins, mimecan is smaller than the other two proteins.[4–6] It would be interesting to know whether the protein-binding properties of KS are affected differently when it is attached to different core proteins.

SLIT-1, -2, and -3 orthologues usually function as chemorepellants of migrating neuronal growth cones.[95] However, an N-terminal fragment of SLIT2, purified from rat brain, causes DRG sensory axons to elongate and branch.[96] Full-length neurorepellant SLIT2 can be transformed into neuroattractant and bifurcation N-terminal SLIT2 by interaction with ECM components,[61] including rat brain heparan sulfate proteoglycan glypican-1(GPC1).[97] Heparan sulfate *O*-sulfate groups are critical for GPC1-SLIT2 binding.[98] The mechanism of the proteolytic SLIT cleavage that results from GPC1-SLIT binding is not yet known. Our protoarray and SPR demonstrations that SLIT2 binds significantly to highly sulfated corneal KS suggests that polyanionic, highly *O*-sulfated ECM KSPG may function as a SLIT2-cleavage facilitator in the cornea, thus converting SLIT2 into its neuroattractant/neurobifurcating form in the area of the developing cornea where corneal nerves are extending and branching extensively.[53,54] This possible chaperone role for polyanionic KS in SLIT2 transformation indeed would mimic the role

of polyanionic regions in other better-known chaperone–protein interactions.[99–101] In addition, under protoarray conditions, ECM neurorepellant SEMA3A was identified as a candidate KS binder. Perhaps association and dissociation constants for SEMA3A with KS could not be determined by SPR because of increased steric hindrance in KS function when it is the moiety attached to the fixed substrate. Our observations suggest that corneal KS is very influential in regulation of corneal innervation during development.

## *References*


1. Gipson IK, Joyce NC, Zieske JD. The anatomy and cell biology of the human cornea, limbus, conjunctiva and adnexa. In: Smolin G, Foster CS, Azar DT, Dohman CH, eds. Smolin and Thoft's The Cornea, Scientific Foundations and Clinical Practice. 4th ed. By Lippincott, Williams, & Wilkins; 2004:3–37.
2. Meyer K, Linker A, Davidson EA, Weissman B. The mucopolysaccharides of bovine cornea. *J Biol Chem.* 1953;205:611–616.
3. Davidson EA, Meyer KJ. Chondroitin, a new mucopolysaccharide. *J Biol Chem.* 1954;211:605–611.
4. Funderburgh JL, Funderburgh ML, Brown SJ, et al. Sequence and structural implications of a bovine corneal keratan sulfate proteoglycan core protein: protein 37B represents bovine lumican and proteins 37A and 25 are unique. *J Biol Chem.* 1993;268:11874–11880.
5. Funderburgh JL, Corpuz LM, Roth MR, et al. Mimecan, the 25-kDa corneal keratan sulfate proteoglycan, is a product of the gene producing osteoglycin. *J Biol Chem.* 1997;272:28089–28095.
6. Corpuz LM, Funderburgh JL, Funderburgh ML, et al. Conrad GW. Molecular cloning and tissue distribution of keratocan: bovine corneal keratan sulfate proteoglycan 37A. *J Biol Chem.* 1996;271:9759–9753.
7. Li W, Vergnes JP, Cornuet PK, Hassell JR. cDNA clone to chick corneal chondroitin/dermatan sulfate proteoglycan reveals identity to decorin. *Arch Biochem Biophys.* 1992;296:190–197.
8. Bianco P, Fisher LW, Young MF, Termine JD, Robey PG. Expression and localization of the two small proteoglycans biglycan and decorin in developing human skeletal and non-skeletal tissues. *J Histochem Cytochem.* 1990;38:1549–1563.
9. Conrad G, Hamilton C, Haynes E. Differences in glycosaminoglycans synthesized by fibroblast-like cells from chick cornea, heart, and skin. *J Biol Chem.* 1977;252:6861–6870.
10. Trelstad RL, Hayashi K, Toole BP. Epithelial collagens and glycosaminoglycans in the embryonic cornea: macromolecular order and morphogenesis in the basement membrane. *J Cell Biol.* 1974;62:815–830.
11. Fitzsimmons TD, Fagerholm P, Harfstrand A, Schenholm M. Hyaluronic acid in the rabbit cornea after excimer laser superficial keratectomy. *Invest Ophthalmol Vis Sci.* 1992;33:3011–3016.
12. Groves ML, McKeon R, Werner E, Nagarsheth M, Meador W, English AW. Axon regeneration in peripheral nerves is enhanced by proteoglycan degradation. *Exp Neurol.* 2005;195:278–292.
13. Manton KJ, Leong DF, Cool SM, Nurcombe V. Disruption of heparan and chondroitin sulfate signaling enhances mesenchymal stem cell-derived osteogenic differentiation via bone morphogenetic protein signaling pathways. *Stem Cells.* 2007;25:2845–2854.
14. Miao HQ, Ishai-Michaeli R, Atzmon R, Peretz T, Vlodavsky I. Sulfate moieties in the subendothelial extracellular matrix are involved in basic fibroblast growth factor sequestration, dimerization, and stimulation of cell proliferation. *J Biol Chem.* 1996;271:4879–4886.
15. Fthenou E, Zafiropoulos A, Tsatsakis A, Stathopoulos A, Karamanos NK, Tzanakakis GN. Chondroitin sulfate A chains enhance platelet derived growth factor-mediated signalling in fibrosarcoma cells. *Int J Biochem Cell Biol.* 2006;38:2141–2150.
16. Fthenou E, Zafiropoulos A, Katonis P, Tsatsakis A, Karamanos NK, Tzanakakis GN. Chondroitin sulfate prevents platelet derived growth factor-mediated phosphorylation of PDGF-Rbeta in normal human fibroblasts severely impairing mitogenic responses. *J Cell Biochem.* 2008;103:1866–1876.
17. Aguiar CB, Lobão-Soares B, Alvarez-Silva M, Trentin AG. Glycosaminoglycans modulate C6 glioma cell adhesion to extracellular matrix components and alter cell proliferation and cell migration. *BMC Cell Biol.* 2005;6:31–39.
18. Cardin AD, Weintraub HJ. Molecular modeling of protein-glycosaminoglycan interactions. *Arteriosclerosis.* 1989;9:21–32.
19. Ruoslahti E, Engvall E. Complexing of fibronectin glycosaminoglycans and collagen. *Biochim Biophys Acta.* 1980;631:350–358.
20. Oldberg A, Ruoslahti E. Interactions between chondroitin sulfate proteoglycan, fibronectin, and collagen. *J Biol Chem.* 1982;257:4859–4863.
21. Funderburgh JL. Keratan sulfate: structure, biosynthesis, and function. *Glycobiology.* 2000;10:951–958.
22. Aplin JD, Hey NA, Graham RA. Human endometrial MUC1 carries keratan sulfate: characteristic glycoforms in the luminal epithelium at receptivity. *Glycobiology.* 1998;8:269–276.
23. Takahashi K, Stamenkovic I, Cutler M, Dasgupta A, Tanabe KK. Keratan sulfate modification of CD44 modulates adhesion to hyaluronate. *J Biol Chem.* 1996;271:9490–9496.
24. Akhtar S, Davies JR, Caterson B. Ultrastructural immunolocalization of alpha-elastin and keratan sulfate proteoglycan in normal and scoliotic lumbar disc. *Spine.* 2005;30:1762–1769.
25. Block JA, Inerot SE, Kimura JH. Heterogeneity of keratan sulfate substituted on human chondrocytic large proteoglycans. *J Biol Chem.* 1992;267:7245–7252.
26. Funderburgh JL, Caterson B, Conrad GW. Keratan sulfate proteoglycan during embryonic development of the chicken cornea. *Dev Biol.* 1986;116:267–277.
27. Funderburgh JL, Funderburgh ML, Rodrigues MM, Krachmer JH, Conrad GW. Altered antigenicity of keratan sulfate proteoglycan in selected corneal diseases. *Invest Ophthalmol Vis Sci.* 1990;31:419–428.
28. Vyas KA, Patel HV, Vyas AA, Wu W. Glycosaminoglycans bind to homologous cardiotoxins with different specificity. *Biochemistry.* 1998;37:4527–4534.
29. Russo VC, Bach LA, Fosang AJ, Baker NL, Werther GA. Insulin-like growth factor binding protein-2 binds to cell surface proteoglycans in the rat brain olfactory bulb. *Endocrinology.* 1997;138:4858–4867.
30. Carlson EC, Lin M, Liu CY, Kao WW, Perez VL, Pearlman E. Keratocan and lumican regulate neutrophil infiltration and corneal clarity in lipopolysaccharide-induced keratitis by direct interaction with CXCL1. *J Biol Chem.* 2007;282:35502–35509.
31. Oki S, Hashimoto R, Okui Y, et al. Sulfated glycosaminoglycans are necessary for Nodal signal transmission from the node to the left lateral plate in the mouse embryo. *Development.* 2007;134:3893–3904.
32. Hindson VJ, Gallagher JT, Halfter W, Bishop PN. Opticin binds to heparan and chondroitin sulfate proteoglycans. *Invest Ophthalmol Vis Sci.* 2005;46:4417–4423.
33. Cortes M, Baria AT, Schwartz NB. Sulfation of chondroitin sulfate proteoglycans is necessary for proper Indian hedgehog signaling in the developing growth plate. *Development.* 2009;136:1697–1706.
34. Maeda N, Fukazawa N, Hata T. The binding of chondroitin sulfate to pleiotrophin/heparin-binding growth-associated molecule is regulated by chain length and oversulfated structures. *J Biol Chem.* 2006;281:4894–4902.
35. Asada M, Shinomiya M, Suzuki M, et al. Glycosaminoglycan affinity of the complete fibroblast growth factor family. *Biochim Biophys Acta.* 2009;1790:40–48.
36. Miyazaki T, Miyauchi S, Tawada A, Anada T, Matsuzaka S, Suzuki O. Oversulfated chondroitin sulfate-E binds to BMP-4 and enhances osteoblast differentiation. *J Cell Physiol.* 2008;217:769–777.
37. Meyer K, Palmer JJ. The polysaccharide of the vitreous humor. *J Biol Chem.* 1934;107:629–634.
38. Hardingham TE, Muir H. The specific interaction of hyaluronic acid with cartilage proteoglycans. *Biochim Biophys Acta.* 1972;279:401–405.
39. LeBaron RG, Zimmermann DR, Ruoslahti E. Hyaluronate binding properties of versican. *J Biol Chem.* 1992;267:10003–10010.

40. Rauch U, Karthikeyan L, Maurel P, Margolis RU, Margolis RK. Cloning and primary structure of neurocan, a developmentally regulated, aggregating chondroitin sulfate proteoglycan of brain. *J Biol Chem.* 1992;267:19536–19547.
41. Yamada H, Watanabe K, Shimonaka M, Yamaguchi Y. Molecular cloning of brevican, a novel brain proteoglycan of the aggrecan/versican family. *J Biol Chem.* 1994;269:10119–10126.
42. Perides G, Lane WS, Andrews D, Dahl D, Bignami A. Isolation and partial characterization of a glial hyaluronate-binding protein. *J Biol Chem.* 1989;264:5981–5987.
43. Lee TH, Wisniewski H-G, Vilcek J. A novel secretory tumor necrosis factor-inducible protein (TSG-6) is a member of the family of hyaluronate binding proteins, closely related to the adhesion receptor CD44. *J Cell Biol.* 1992;116:545–557.
44. Aruffo A, Stamenkovic I, Melnick M, Underhill CB, Seed B. CD44 is the principal cell surface receptor for hyaluronate. *Cell.* 1990; 61:1303–1313.
45. Kohda D, Morton CJ, Parkar AA, et al. Solution structure of the link module: a hyaluronan-binding domain involved in extracellular matrix stability and cell migration. *Cell.* 1996;86:767–775.
46. Yamada KM, Kennedy DW, Kimata K, Pratt RM. Characterization of fibronectin interactions with glycosminoglycans and identification of active proteoplytic fragments. *J Biol Chem.* 1980;255: 6055–6063.
47. Sohr S, Engeland K. RHAMM is differentially expressed in the cell cycle and downregulated by the tumor suppressor p53. *Cell Cycle.* 2008;7:3448–3460.
48. Day AJ, Prestwich GD. Hyaluronan-binding proteins: tying up the giant. *J Biol Chem.* 2002;277:4585–4588.
49. Gustafson S, Bjork T, Forsberg N, Lind T, Wikstrom T, Lidholt K. Accessible hyaluronan receptors identical to ICAM-1 in mouse mast-cell tumors. *Glycoconj J.* 1995;12:350–355.
50. Evanko SP, Wight TN. Intracellular localization of hyaluronan in proliferating cells. *J Histochem Cytochem.* 1999;47:1331–1342.
51. Collis L, Hall C, Lange L, Ziebell M, Prestwich R, Turley EA. Rapid hyaluronan uptake is associated with enhanced motility: implications for an intracellular mode of action. *FEBS Lett.* 1998;440: 444–449.
52. Lwigale PY, Bronner-Fraser M. Lens-derived Semaphorin3A regulates sensory innervation of the cornea. *Dev Biol.* 2007;306:750–759.
53. Conrad AH, Strafuss JM, Wittman MD, Conway S, Conrad GW. Thyroxine increases the rate but does not alter the pattern of innervation during embryonic chick corneal development. *Invest Ophthalmol Vis Sci.* 2008;49:139–153.
54. Conrad AH, Albrecht M, Pettie-Scott M, Conrad GW. Embryonic corneal Schwann cells express some Schwann cell marker mRNAs, but no mature Schwann cell marker proteins. *Invest Ophthalmol Vis Sci.* 2009;50:4173–4184.
55. Osmond RI, Kett WC, Skett SE, Coombe DR. Protein-heparin interactions measured by BIAcore 2000 are affected by the method of heparin immobilization. *Anal Biochem.* 2002;310: 199–207.
56. Saito A, Munakata H. Detection of chondroitin sulfate-binding proteins on the membrane. *Electrophoresis.* 2004;25:2452–2460.
57. Müller LJ, Marfurt CF, Kruse F, Tervo TM. Corneal nerves: structure, contents and function. *Exp Eye Res.* 2003;76:521–542.
58. Brose K, Bland KS, Wang KH, et al. Slit proteins bind Robo receptors and have an evolutionarily conserved role in repulsive axon guidance. *Cell.* 1999;96:795–806.
59. Hirst CE, Ng ES, Azzola L, et al. Transcriptional profiling of mouse and human ES cells identifies SLAIN1, a novel stem cell gene. *Dev Biol.* 2006;293:90–103.
60. Ma L, Tessier-Lavigne M. Dual branch-promoting and branch-repelling actions of Slit/Robo signaling on peripheral and central branches of developing sensory axons. *J Neurosci.* 2007;27: 6843–6852.
61. Nguyen-Ba-Charvet KT, Brose K, Marillat V, Sotelo C, Tessier-Lavigne M, Checlotal A. Sensory axon response to substrate-bound Slit2 is modulated by laminin and cyclin GMP. *Mol Cell Neursci.* 2001;17:1048–1058.
62. González-Romero FJ, Gragera RR, Martínez-Murillo R, Martínez-Rodríguez R. Cytochemical and immunocytochemical comparative localization and characterization of acid sulfated glycolaminoglycans (sGAG) in several areas of the rat cerebral cortex during postnatal development. *J Hirnforsch.* 1994;35:511–520.
63. Schafer IA, Sorrell JM. Human keratinocytes contain keratin filaments that are glycosylated with keratan sulfate. *Exp Cell Res.* 1993;207:213–219.
64. Ohmori J, Nawa Y, Yang DH, Tsuyama S, Murata F. Keratan sulfate glycosaminoglycans in murine eosinophil-specific granules. *J Histochem Cytochem.* 1999;47:481–488.
65. Nakamura H, Hirata A, Tsuji T, Yamamptp T. Immunolocalization of keratan sulfate proteoglycan in rat calvaria. *Arch Histol Cytol.* 2001;64:109–118.
66. Cohen RJ, Holland JW, Redmond SL, McNeal JE, Dawkins HJS. Identification of the glycosaminoglycan keratan sulfate in the prostatic secretory cell. *Prostate.* 2000;44:204–209.
67. Marson A, Robinson DE, Brookes PN, et al. Development of a microtiter plate-based glycosaminoglycan array for the investigation of glycosaminoglycan-protein interactions. *Glycobiology.* 2009;19:1537–1546.
68. Wang DN, Liu SY, Trummer BJ, Deng C, Wang AL. Carbohydrate microarrays for the recognition of cross-reactive molecular markers of microbes and host cells. *Nat Biotech.* 2002;20:275–281.
69. Saito A, Munakata H. Factor H is a dermatan sulfate-binding protein: identification of a dermatan sulfate-mediated protease that cleaves factor H. *J Biochem.* 2005;137:225–233.
70. Marson A, Rock MJ, Cain SA, et al. Homotypic fibrillin-1 interactions in microfibril assembly. *J Biol Chem.* 2005;278:41205–41212.
71. Yang B, Yang BL, Goetinck PF. Biotinylated hyaluronic acid as a probe for identifying hyaluronic acid-binding proteins. *Anal Biochem.* 1995;228:299–306.
72. Parkar AA, Day AJ. Overlapping sites on the Link module of human TSG-6 mediate binding to hyaluronan and chondroitin 4-sulfate. *FEBS Lett.* 1997;410:413–417.
73. Watanabe H, Cheung SC, Itano N, Kimata K, Yamata Y. Identification of hyaluronan-binding domains of aggrecan. *J Biol Chem.* 1997;272:28057–28065.
74. Laterra J, Culp LA. Differences in the hyaluronate binding to plasma and cell surface fibronectins: requirement for aggregation. *J Biol Chem.* 1982:257;719–726.
75. Arai T, Busby W, Clemmons DR. Binding of insulin-like growth factor (IGF) I or II to IGF-binding protein-2 enables it to bind to heparin and extracellular matrix. *Endocrinology.* 1996;11:4571–4575.
76. Nadesalingam J, Bernal AL, Dadds AW, et al. Identification and characterization of a novel interaction between pulmonary surfactant protein D and decorin. *J Biol Chem.* 2003;278:25678–25687.
77. Mahoney DJ, Mulloy B, Forster MJ, et al. Characterization of the interaction between tumor necrosis factor-stimulated gene-6 and heparin: implications for the inhibition of plasmin in extracellular matrix microenvironments. *J Biol Chem.* 2005;280:27044–27055.
78. Harris EN, Weigel JA, Weigel PH. The human hyaluronan receptor for endocytosis (HARE/Stabilin-2) is a systemic clearance receptor for heparin. *J Biol Chem.* 2008;283:17341–17350.
79. Boucas RI, Trindade ES, Tersariol IL, Dietrich CP, Nadar HB. Development of an enzyme-linked immunosorbent assay (ELIZA)-like fluorescence assay to investigate the interactions of glycosaminoglycans to cells. *Anal Chim Acta.* 2008;618: 218–226.
80. Zhang F, McLellan JS, Ayala AM, Leahy DJ, Linhardt RJ. Kinetic and structural studies on interactions between heparin or heparan sulfate and proteins of the Hedgehog signaling pathway. *Biochemistry.* 2007;46:3933–3941.
81. Tai G-H, Nieduszynski IA, Fullwood NJ, Huckerby TN. Human corneal keratan sulfates. *J Biol Chem.* 1997;272:28227–28231.
82. Achur RN, Muthusamy A, Madhunapantula SV, Bhavanandan VP, Seudieu C, Gowda DC. Chondroitin sulfate proteoglycans of bovine cornea: structural characterization and assessment for the adherence of Plaqsmodium faciparum-infected erythrocytes. *Biochim Biophsy Acta.* 2004;1701:109–119.

83. Plaas AH, West LA, Thonar EJA, et al. Altered fine structure of corneal and skeletal keratan sulfate and chondroitin/dermal sulfate in macular corneal dystrophy. *J Biol Chem.* 2001;276:39788–39796.
84. Achur RN, Kakizaki I, Goel S, et al. Structural interactions in chondroitin 4-sulfate mediated adherence of Plasmodium falciparum infected erythrocytes in human placenta during pregnancy-associated malaria. *Biochemistry.* 2008;47:12635–12643.
85. Gama CI, Tully SE, Sotogaku N, et al. Sulfation patterns of glycosaminoglycans encode molecular recognition and activity. *Nature Chem Biol.* 2006;2:467–473.
86. Hileman RE, Fromm JR, Weiler JM, Linheardt RJ. Glycosaminoglycan-protein interactions: definition of consensus sites in glycosaminoglycan binding proteins. *BioEssays.* 1998;20:156–167.
87. Salamat-Miller N, Fang J, Seidel CW, et al. A network-based analysis of polyanion-binding proteins utilizing yeast protein arrays. *Mol Cell Proteomics.* 2006;5:2263–2278.
88. Salamat-Miller N, Fang J, Seidel CW, Assenov Y, Albrecht M, Middaugh CR. A network-based analysis of polyanion-binding proteins utilizing human protein arrays. *J Biol Chem.* 2007;282:10153–10163.
89. Jones LS, Yazzie B, Middaugh CR. Polyanions and the proteome. *Mol Cell Proteomics.* 2004;3:746–769.
90. Wright PE, Dyson HJ. Intrinsically unstructured proteins: re-assessing the protein structure-function paradigm. *J Mol Biol.* 1999;293:321–331.
91. Hanks SK, Quinn AM. Protein kinase catalytic domain sequence database: identification of conserved features of primary structure and classification of family members. *Methods Enzymol.* 1991;200:38–62.
92. Rogers MA, Langbein L, Winter H, Ehmann C, Praetzel S, Schweizer J. Characterization of a first domain of human high glycine-tyrosine and high sulfur keratin-associated protein (KAP) genes on chromosome 21q22.1. *J Biol Chem.* 2002;277:48993–49002.
93. Wu A, Chen J, Baserga R. Nuclear insulin receptor substrate-1 activates promoters of cell cycle progression genes. *Oncogene.* 2008;27:397–403.
94. Araki E, Sun XL, Haag BL, et al. Human skeletal muscle insulin receptor substrate-1: characterization of the cDNA, gene, and chromosomal localization. *Diabetes.* 1993;42:1041–1054.
95. Li HS, Chen JH, Wu W, et al. Vertebrate slit, a secreted ligand for the transmembrane protein roundabout, is a repellent for olfactory bulb axons. *Cell.* 1999;96:807–818.
96. Wang KH, Brose K, Arnott D, et al. Biochemical purification of a mammalian slit protein as a positive regulator of sensory axon elongation and branching. *Cell.* 1999;96:771–784.
97. Liang Y, Annan RS, Carr SA, et al. Mammalian homologues of the Drosophila Slit protein are ligands of the heparan sulfate proteoglycan glypican-1 in brain. *J Biol Chem.* 1999;274:17885–17892.
98. Ronca F, Anderson JS, Paech V, Margolis RU. Characterization of Slit protein interactions with Glypican-1. *J Biol Chem.* 2001;276:29141–29147.
99. Edwards KL, Kueltzo LA, Fisher MT, Middaugh CR. Complex effects of molecular chaperones on the aggregation and refolding of fibroblast growth factor-1. *Arch Biochem Biophys.* 2001;393:14–21.
100. Park SM, Jung HY, Kim TD, Park JH, Yang CH, Kim J. Distinct roles of the N-terminal-binding domain and the C-terminal-solubilizing domain of alpha-synuclein, a molecular chaperone. *J Biol Chem.* 2002;277:28512–28520.
101. Hingorani K, Szebeni A, Olson MO. Mapping the functional domains of nucleolar protein B23. *J Biol Chem.* 2000;275:24451–24457.